Identification of novel small-molecule inhibitors of ETS-related gene (ERG) oncoproteins as potential anti-prostate cancer agents

by

Ka Yee Chan

Master of Science

Department of Medicine, Division of Experimental Medicine

McGill University

Montreal, Quebec

December 2013

A thesis submitted to McGill University in partial fulfillment of the requirements for the degree of Master of Science

TABLE OF CONTENTS

ABSTRACT

More than 30,000 men in North America annually die from prostate cancer. Currently, mainstay therapy for advanced prostate cancer is to suppress androgen receptor (AR) signaling. Since AR can be activated via multiple mechanisms, inhibition of one or two of these mechanisms is typically initially effective, but drug resistance can rapidly develop due to kick-in of other AR-activating mechanisms, resulting in incurable castration-resistant prostate cancer (CRPC). Therefore, the therapeutic effects of most currently available AR-targeting agents are short-lived. To achieve long lasting therapeutic effect for prostate cancer, it appears we need to get out of the box of AR. Here, we propose to develop chemical inhibitors of oncogenic protein ERG, which is an ETS transcriptional factor. The rationale for inhibiting ERG as a possible treatment for prostate cancer is of two folds: 1) ERG plays a critical role in prostate cancer initiation and progression, and 2) Half of all prostate cancer patients are TMPRSS2-ERG fusion positive, which result in high level of ERG oncoprotein. ERG is a transcriptional factor that directly regulates EZH2, c-Myc, and the tumor suppressor NKX3.1 and many other targets in prostate cancer. ERG cooperates with PI3K/AKT and AR in tumor initiation. ERG knockdown inhibits tumor growth in xenograft of VCaP cells.

In this thesis, my goal was to discover novel small-molecule inhibitors of ERG as anti-prostate cancer agents. I have built a structural model of ERG DNA-binding domain and performed virtual screening studies against National Cancer Institute chemical database and our in-house chemical database. I have discovered a novel compound called **V131**, which substantially inhibits ERG-dependent reporter activity in HEK293 cells. **V131** inhibits invasion of VCaP cells (TMPRSS2-ERG positive), but not the DU145 cells (TMPRSS2-ERG negative) in Boyden chamber invasion assay. Importantly, our lab has also discovered a novel in-house

synthetic compound referred to as **#648** that potently inhibits ERG transcriptional activity, and invasion of VCaP cells but not DU145 cells. Furthermore, surface plasmon resonance analysis has confirmed direct binding of **#648** and recombinant human ERG protein. TMPRSS2-ETV1 is also found in advanced PCa patients. Alongside, I have identified another novel compound **V154**, which showed substantial inhibitory activity against ETV1.

AR inhibitors capable of effectively suppressing the sustained AR signaling in CRPC cells has been a major challenge in the field. Metastatic disease presents a continuing therapeutic challenge and is the most common cause of cancer-related deaths. As recent studies indicated that localized PCa with TMPRSS2-ERG positive is prone to lymph node metastasis, ERG inhibitor could potentially prevent patients with localized PCa from progression to metastatic PCa. Our future work will focus on further characterization of the mechanism of action and chemical optimization of our lead compounds **V131**, **V154** and **#648**.

Résumé

Chaque année, plus de 30, 000 hommes meurent du cancer de la prostate en Amérique du Nord. Actuellement, la suppression de la voie de signalisation du récepteur à l'androgène (AR) constitue la principale option thérapeutique dans les cas avancés du cancer de la prostate. Une résistance aux inhibiteurs d'AR peut apparaître rapidement si la tumeur développe des mécanismes activant le récepteur AR indépendamment de la liaison avec son ligand. De telles tumeurs sont appelées cancers de la prostate résistants à la castration et sont responsables pour la majeure partie de la mortalité associée au cancer de la prostate. Une résistance à la castration apparaît relativement tôt dans la progression du cancer de la prostate, ce qui limite la durée d'efficacité des inhibiteurs d'AR. Il semble donc nécessaire de trouver des alternatives afin d' améliorer l' efficacité thérapeutique à long-terme. Nous proposons de développer une voie alternative ciblant l'oncogène ERG, un facteur de transcription régulant des gènes importants dans la formation de métastases tels que EZH2 et c-Myc. De nombreuses études ont montré que la surexpression de ERG est associée avec une augmentation de la capacité des cellules à proliférer et à envahir d'autres tissus. ERG est utilisé comme cible thérapeutique afin de traiter le cancer de la prostate pour les raisons suivantes. 1) ERG joue un rôle critique lors de l'initiation et la progression du cancer de la prostate. 2) La moitié des patients souffrant du cancer de la prostate possède la fusion TMPRSS2-ERG, ce qui conduit à des niveaux élevés de la forme oncogénique de ERG. ERG coopère avec PI3K/AKT et AR lors de l'initiation de la tumeur.

Au cours ma thèse, mon objectif fut de découvrir et caractériser de nouveaux inhibiteurs de ERG possédant des propriétés anti-tumorales. J'ai construit un modèle structurel du domaine de liaison à l'ADN de ERG, et après avoir examiné *in silico* la base de donnée de composés chimiques du National Cancer Institut et la base de donnée de notre laboratoire, j'ai pu identifier

une molécule **(V131)** capable d'inhiber l'activité de ERG dans un système rapporteur luciférase dans les cellules HEK293. **V131** a montré une inhibition importante du potentiel invasif des cellules VCaP (TMPRSS2-ERG positive) mais n'a pas eu d'effet sur les cellules DU145 (TMPRSS2-ERG négative). Parallèlement, un autre composé **(V154)** capable d'inhiber cette fusion dans des expériences de système rapporteur luciférase a été identifié. Le composé **#648** synthétisé dans notre laboratoire a montré des résultats identiques à ceux obtenus avec le composé **V131**. De plus, des expériences de résonance des plasmons de surface ont confirmé la liaison directe entre **#648** et la protéine ERG. En parallèle, j'ai pu montrer que le composé **V154** possédait aussi une activité inhibitrice contre ETV1.

La mise au point d'inhibiteurs d'AR capable d'inhiber efficacement la voie de signalisation d' AR dans les cellules CRPR est un des principaux défis du domaine. L'apparition de métastases représente un obstacle et est la principale cause de décès pour les patients atteints de cancer. De récentes études ont montré que les cancers de la prostate surexprimant la fusion TMPRSS2-ERG avaient plus de risque de métastaser au niveau des ganglions lymphatiques. Les inhibiteurs de ERG pourraient potentiellement prévenir l'apparition de ces métastases. Nos travaux futurs vont se concentrer sur la caractérisation plus approfondie du mécanisme d'action des nouveaux composés identifiés : **V131**, **V154** et **#648**.

DEDICATION

TO MY DEAR PARENTS AND FRIENDS.

ACKNOWLEDGMENTS

I thank Dr. Jian Hui Wu for his supervision and guidelines. Our lab technician, Ms. Guoyan Geng has to be acknowledged that she helped of my cell cultures when I was out of town. I thank Dr. Xiaohong Tian, a postdoc fellow for synthesizing chemical compounds in my project, including design and synthesis of compound **#648**. McGill's Surface Plasma Resonance Facility contributed efforts to confirm the direct binding of our compounds.

The committee members, Drs. Rongtuan Lin, Andrew Mouland, and Ivan Topisirovic (last name in alphabet order) are helpful to foster my development in molecule biology and medical research. I give many thanks to their time and expertise.

My working bench is surrounded by the labs of Drs. Moulay Alaoui-Jamali, Gerald Batist, Rongtuan Lin, and Michael Witcher (last name in alphabet order). I thank them for generous offers using their lab equipments. Their lab members are very capable and helpful. They have made an enjoyable working environment.

For the translation of my abstract to French, it was kindly helped by Dr. Maud Marques, Dr. Khalid Hilmi, and Gregoire Morand, MD. I greatly appreciate their helps and time. I have to thank our student affair staff members in Divison, Ms. Dominique Besso and Ms. Marylin Linhares for smoothing my graduation process.

My sincere gratitude also has to go to the McGill CIHR (Canadian Institutes of Health Research) Drug Development Training awarded me a one-year fellowship to aid my study financially. This project was funded by Prostate Cancer Canada via a Movember discovery grant (to J. Wu).

I know money makes most of things possible and I am truly grateful for the financial support during my study. Nevertheless, your blessings, care, encouragement, love and warm

regards, even your complaints are vital for my breath and life: My dear family and friends. All of you are remarkably important during my time studying abroad, as well as to my personal growth beyond scientific research. Not to mention your invitation for dinner is so heart-warming to me. Although I cannot mention all of your names, each one of you has unique influence to my growth. I thank all of you for all forms of support throughout the entire process.

LIST OF TABLES

LISTS OF FIGURES

ABBREVIATIONS

ACTH	Adrenocorticotropic hormone
ADT	Androgen deprivation therapy
AR	Androgen receptor
cDNA	Complementary deoxyribonucleic acid
CoIP	Co-immunoprecipitation
CRPC	Castration resistance prostate cancer
CYP17	Cytochrome P450 17
DBD	DNA binding domain
DHT	Dihydrotestosterone
DMEM	Dulbecco's modified eagle's medium
DMSO	Dimethyl sulfoxide
DNA	Deoxyribonucleic acid
DNA-PKs	DNA-dependent protein kinase, catalytic subunits
ELF3	E74-like factor-3
ELISA	Enzyme-linked immunosorbent assay
ELK4	ETS domain-containing protein Elk-4
ERG	ETS-related gene
ETS	E26 transformation-specific sequence
ETS1	E26 oncogene homolog 1
ETS2	E26 oncogene homolog 2
ETV	ETS translocation variant
EWS-FLI1	Ewing's sarcoma-Friend leukemia integration 1
EZH2	Enhancer of zeste homology 2
FBS	Fetal bovine serum
FDA	The U.S. Food and Drug Administration
FSH	Follicle-stimulating hormone
GnRH	Gonadotropin-releasing hormone
HBS	HEPES buffered saline
HEPES	4-(2-hydroxyethyl)-1-piperazineethanesulfonic acid
IC50	Half maximal inhibitory concentration
LBD	Ligand binding domain
LH	Luteinizing hormone
LHRH	Luteinizing hormone-releasing hormone
mRNA	Messenger ribonucleic acid
MTT	Methyl thiazolyl diphenyl tetrazolium bromide
NCI	National Cancer Institute
NMR	Nuclear magnetic resonance

NP-40	Tergitol-type nonyl phenoxypolyethoxylethanol-40
NT	Vehicle control
OD	Optical density
PARP1	Poly [Adenosine-diphosphate-ribose] polymerase 1
PCa	Prostate cancer
PDB	Protein Data Bank
PI3K	Phosphatidylinositide 3-kinases
PIN	Prostate intraepithelial neoplasia
PNT	Pointed
PSA	Prostate specific antigen
PTEN	Phosphatase and tensin homolog
PVDF	Polyvinylidene difluoride
qPCR	Quantitative polymerase chain reaction
RLU	Relative light unit
RPMI	Roswell Park Memorial Institute
RT-PCR	Reverse transcription polymerase chain reaction
SCID	Severe combined immunodeficiency
SDS-PAGE	Sodium dodecyl sulfate-polyacrylamide gel electrophoresis
shRNA	Short hairpin ribonucleic acid
siRNA	Small interfering ribonucleic acid
SPR	Surface plasmon resonance
TBS-T	Tris-buffered saline-Tween 20
TMPRSS2	Transmembrane protease, serine 2

CHAPTER 1. BACKGROUND, RATIONALE AND OBJECTIVES

1.1. Prostate cancer

Prostate cancer (PCa) is a heterogeneous, multi-factorial disease with genetic alternations and environmental factors perplexed in its etiology. However, the key molecular mechanisms responsible for the initiation and progression of PCa remain largely under investigation. PCa is the most common diagnosed solid non-skin tumor in men worldwide, with high number of cases in the United States, Western Europe [1]. The incidence of PCa in Asia is on the rise [2, 3]. Risk factors of PCa were found associated with age, family history, and ethnicity [4-6]. Like many other types of cancer, early detection of PCa can significantly improve patient survival rate. Prostate specific antigen (PSA) testing and Gleason score on biopsy are currently in use to stratify patients into risk groups [7, 8]. Nevertheless they are not reliable enough to distinguish localized cancer from aggressive cancer, which often leads to over-diagnosis and subsequently causes large amounts of unnecessary treatments [9].

Over the last 5 years, age-adjusted PCa deaths have been decreasing **(Figure 1.1)** [37]. Nevertheless, PCa is the second leading cause of cancer death in men [38]. In 2013, Canadian Cancer Society estimated that 23,600 men will be diagnosed with PCa in Canada, whereas 3,900 men would die from PCa. About one in seven Canadian men is expected to develop PCa during his lifetime and one in 28 men will die from it. In USA, it was predicted that 28,170 men would die from prostate cancer in 2012 [1]. About one in six American men will be diagnosed with PCa during his lifetime. It is clear that PCa remains a serious medical health issue.

1.2. Current treatment options for prostate cancer and the limitations

1.2.1. Current treatment options for prostate cancer

Current treatments of clinically localized PCa include digital rectal examination, radical prostatectomy and radiotherapy, which provide high survival rates in localized PCa men [10]. For locally advanced PCa with extracapsular extension of the tumor, radiotherapy remains the standard treatment [11].

Charles Huggins's work establishing that PCa was androgen dependent and could be treated by castration earned him the Nobel Prize [10]. Androgen-deprivation therapy (ADT) has been the mainstay treatment of metastatic prostate cancer since 1940s [12]. ADT is to suppress the AR signaling by surgical or chemical castration to reduce the production of the male sex hormone testosterone. Chemical castration is done by GnRH agonists or antagonists. As shown in **Figure 1.2**, GnRH agonists initially increase testosterone levels briefly and then result in low testosterone levels through a feedback loop. On the other hand, GnRH antagonists reduce testosterone levels more quickly and avoid initial surging of the testosterone level. In addition, ADT is frequently combined with antiandrogens, such as bicalutamide, which inhibit binding of androgens to the AR ligand-binding domain (LBD). Flutamide, nilutamide and bicalutamide are nonsteroidal antiandrogens that are currently used in the clinic **(Figure 1.3)** [13]. Despite of initial response to ADT and conventional antiandrogens, most of patients progress to an incurable status called castration-resistance prostate cancer (CRPC). Current treatment modalities for CRPC are limited to docetaxel-based chemotherapy, which provides only a modest improvement in overall patient survival (few months) [14, 15].

Abiraterone and enzalutamide were recently approved by the U.S. Food and Drug Administration (FDA) as oral agents for CRPC patients **(Figure 1.4)**. They can improve overall survival by a few months [12, 13]. Abiraterone is a potent inhibitor of 17α-hydroxylase/ 17,20-

lyase, a key enzyme for androgen synthesis **(Figure 1.5)** [16]. Enzalutamide is a second-generation antiandrogen with stronger binding affinity to the AR than bicalutamide [17]. Enzalutamide inhibits nuclear translocation of the AR and is an antagonist of the W741C mutated AR [17, 18]. In phase III clinical trials, abiraterone and enzalutamide have extended the overall survival of CRPC patients by 4.6 and 4.8 months [19, 20], respectively.

1.2.2. The limitations of androgen receptor-targeting modalities for prostate cancer

As mentioned earlier, most patients under ADT therapy still progress to a more aggressive and incurable disease status called castration resistance prostate cancer (CRPC) [21]. The efficacy of abiraterone and enzalutamide in CRPC patients has revealed that most CRPC cells remain hormone-driven [18, 22]. However, reports to date suggest that resistance to abiraterone and enzalutamide invariably develops within 1-3 years and is characterized with a rising serum prostate-specific antigen (PSA), suggesting aberrant reactivation of the AR signaling [22-24]. Recently, the F876L mutation in AR-LBD has been found to confer enzalutamide resistance, and worse yet, enzalutamide becomes an agonist of the F876L mutated AR [25, 26].

Intensive research studies have unraveled multiple possible mechanisms that may account for aberrant AR reactivation in the CRPC cells: 1) Elevated expression of AR driven by gene amplification [27, 28]; 2) AR gene mutations that result in mutated ARs that could be activated by a broader range of ligands, even antiandrogens [29, 30]; 3) Increased intratummoric androgen synthesis [31]; 4) Increased expression of coactivators [32, 33]; 5) Expression of androgen receptor variants lacking ligand-binding domain (LBD) [34, 35], and 6) Androgen-independent activation of the AR via cross-talk with growth factors and cytokines [36] in CRPC patients. Thus, inhibition of one or two of these AR-activating mechanisms might be initially effective, but

drug resistance could rapidly develop due to kick-in of other AR-activating mechanisms. Persistent recurrent AR signaling remains a driver of CRPC. Therefore, it is highly desirable to explore non-AR- targeting therapies.

1.3. TMPRSS2-ETS gene fusions in prostate cancer

1.3.1. Discovery of TMPRSS2-ERG, TMPRSS2-ETV1, and TMPRSS2-ETV4 in prostate cancer

The ETS related gene (ERG) is a transcriptional factor. In 2005 Chinnaiyan's research group used cancer outlier profile analysis to survey 132 gene-expression PCa datasets from the Oncomine database (Compendia Bioscience). Two erythroblastosis virus E26 transformation-specific (ETS) transcription factors, ETS variant 1 (ETV1, 7p21.3) and ETS-related gene (ERG, 21q22.2), were identified as high-ranking outliers in several independent gene-expression profiling datasets [27]. This study reported 92% of radical prostatectomy samples (23/29 samples) harbored a fusion of the 5' untranslated region of TMPRSS2 with the coding sequences of either ERG or ETV1 (referred to as TMPRSS2-ERG and TMPRSS2-ETV1, respectively) [37]. Shortly thereafter, the fusion gene of TMPRSS2-ETV4 was identified in PCa [38].

TMPRSS2 is a transmembrane serine protease and it is regulated by the AR. Importantly, it is the promoter region of TMPRSS2 that is fused with ERG, ETV1 or ETV4 **(Figure 1.6)**. Importantly, because TMPRSS2 is a target of the AR, the TMPRSS2-ERG fusion results in regulation of ERG expression by AR signaling **(Figure 1.7)**.

1.3.2. Prevalence of TMPRSS2-ETS gene fusions in prostate cancer

The TMPRSS2-ERG gene fusion is found in approximately 50% of Caucasian localized PCa patients and in similar percentage of metastatic PCa patients [39, 40]. But this fusion gene is with a lower reported frequency in African-American men and is less common in Asian cohorts [41-44]. However, more subsequent studies showed TMPRSS2-ERG gene fusion was exceptionally variable and inconsistent in the literature, ranging from 27% to 79% in radical prostatectomy and biopsy samples, generally from PSA screened cohorts among different ethnic groups [37, 42, 45-48]. Aberrant expression of ERG also occurs in Ewing's sarcoma and acute myeloid leukemia [28, 29].

1.4. ERG is an oncogenic protein

A series of studies indicated that expression of ERG enhances cell invasion *in vitro* and induces prostate intraepithelial neoplasia (PIN) in mouse models [30-32]. It was demonstrated that ERG cooperates with loss of PTEN to promote PCa progression in mouse models [33, 34]. Knockdown of ERG resulted in inhibition of xenograft tumor growth of VCaP prostate cancer cells, which is TMPRSS2-ERG positive. Overall, accumulating evidences suggest that ERG could be a promising therapeutic target for PCa.

1.4.1. ERG structure and functions

The human ERG and FLI1 are ETS family members and share 96% homologous to each other [49]. Human ERG was first cloned in 1987 [50]. ERG is a transcription factor. Full-length

ERG contains one pointed (PNT) domain (residues 120-206) and one ETS DNA binding domain (DBD) (residues 318-398) **(Figure 1.8 A)** [51, 52]. To date, the NMR structure of PNT domain is available (PDB entry: 1sxe), but there is no functional sites for the design of inhibitors. The crystal structure of ERG DBD was not available until January 2013 (PDB entry: 4irg) [53].

The pointed (PNT) domain is the second most conserved domain found in ETS genes. Of the 28 human ETS genes, only 11 contain a PNT domain. This domain forms a helix-loop-helix structure which can dimerize with other proteins [54, 55]. The conserved ETS DBD consists of three α–helices on a small four-stranded, antiparallel β–sheet scaffold [56-58]. This DBD domain binds directly to the major-groove DNA over a region covering 12 – 15 base pairs, focused in the region of the 5'-GGA(A/T)-3' sequence motif. Interaction with this DNA sequence is mediated by hydrogen bonding with the two guanine of the GGA(A/T) core. All 28 human ETS genes and all PCa and Ewing's sarcoma derived ETS gene fusions contain an ETS DNA binding domain.

The biological functions of ERG have been examined in xenopus, zebra fish, and mouse and primary prostate cancer cells [59-65]. In mouse models, ERG was found to regulate the normal platelet development, stem-cell function, definitive hematopoiesis and the normal megakaryopoiesis [65, 66]. ERG is shown to be a critical early regulator of fetal hematopoietic stem cell maintenance, and is therefore required to sustain definitive hematopoiesis [66]. On the other hand, ERG has been found to directly regulate a series of targets that are critical for PCa progression. These findings could be summarized as follows: 1) ERG promotes epithelial to mesenchymal transition in immortalized prostate epithelial cell through the ZEB1/ZEB2 axis [67]; 2) ERG promotes invasiveness and migration of PCa cells by upregulating expression of EZH2, CXCR4, ADAM19, PLAU, PLAT, PLA1A, ostepontin, MMP1, MMP3 and MMP9 [68-71]; 3) ERG regulates prostate inflammation via HPGD, NK-κB and TLR4 [72, 73]; 4) ERG

regulates PCa cells' epigenetic reprogramming through EZH2, HAT and HDACs [71, 74]; 5) ERG inhibits a number of prostate differentiation genes such as SLC45A3/Prostein and abrogates the prostate epithelial differentiation program [59, 75]; and 6) ERG upregulates c-Myc oncogene and down-regulates tumor-suppressor NKX3.1 expression in PCa cells [59, 71].

1.4.2. *In vitro* studies

In cellular models, knockdown of ERG by siRNA in VCaP cells substantially inhibits their invasiveness and proliferation [59, 75]. Conversely, ERG overexpression in normal prostate cell line, PrEC, was found to increase invasiveness [75] and proliferation rates [61]. In addition, ERG overexpression in normal epithelial cells RWPE and PNT1a, and benign prostatic hyperplasia epithelial cells BPH-1 was found to substantially increase their invasiveness and cellular migration [61, 76].

1.4.3. *In vivo* studies

In mouse models, ERG overexpression induces PCa progression. Carver *et al.* showed that aberrant ERG expression cooperates with loss of PTEN to promote cancer progression [77]. Importantly, Yang *et al.* demonstrated strong *in vivo* synergistic effects between high levels of ERG and enhanced AR signaling or aberrant PI3K pathway. Moreover, combined AR and ERG overexpression, but not the AR overexpression alone, resulted in the progression of ERG-induced PIN lesions to invasive adenocarcinoma [78]. Alternatively, when ERG knockdown using siRNA in VCaP cells in xenograft model, only 2 out 9 of the ERG siRNA SCID mice

developed tumors, compared to 5 out of 5 SCID mice in the control group [59]. A study using shRNA ERG demonstrated that loss of ERG expression causes a loss in proliferation of hematopoietic cells [79, 80] and ectopic expression of ERG in fetal hematopoietic progenitors was shown to promote megakaryopoiesis and induce rapid-onset leukemia when transplanted into sub-lethally irradiated syngeneic mice [80]. These studies indicate ERG is oncogenic and ERG could be a drug target for PCa, and possibly for leukemia.

1.4.4. Clinical evidences

In patients, TMPRSS2-ERG status has been linked to poor outcomes and PCa specific death [81-83]. Fusion positive prostate cancers have been associated with high grade tumors [46], and are prone to metastasis [84, 85]. In particular, Perner *et al.* [84] and Gao *et al.* [86] have found that localized PCa with TMPRSS2-ERG fusion have greater predilection for lymph node metastasis. Bismar *et al.* found that ERG protein expression reflected hormonal treatment response and was associated with Gleason score and PCa specific death [87]. Spencer *et al.* showed that the relative intensity and composite score for ERG expression was prognostic for the development of biochemical relapse, metastases, and prostate cancer-specific mortality [88].

1.5. Other ETS transcription factors play a role in prostate cancer

The human ETS family of transcription factors consists of 28 evolutionarily related genes in humans that control unique transcriptional process by binding to the specific DNA recognition sequence 5'-GGA(A/T)-3' and by recruiting transcriptional machinery [89]. ETS genes have roles in cellular proliferation, differentiation, development, transformation, and apoptosis [90,

91]. ETS transcriptional factors contain a conserved "ETS DNA binding domain (DBD)". Most ETS members contain a second conserved domain called "pointed domain" [89].

FLI1, ETS2 and ELF3 are ETS transcriptional factors. In Ewing's sarcomas, EWS gene 22 is aberrantly juxtaposed to FLI1 and it is frequently found in highly aggressive small round blue cell malignancies of the bone and soft tissue [92]. ETS2 contributes to neoplastic transformation and maintenance of the malignant phenotype in various cancer types, including prostate, breast and thyroid cancers [93-97]. Whereas, ELF3 is a repressor of androgen receptor action in PCa cells [98]. Exogenous expression of ELF3 represses AR transcriptional activity when was assessed using reporter assays. The interaction between endogenous ELF3 and AR was demonstrated through co-immunoprecipitation (CoIP) assay in LNCaP cells.

1.6. Current small-molecule inhibitors of ETS transcription factors

In 2009, Erkian *et al.* identified a compound YK-4-279 **(Figure 1.9)** that binds with EWS-FLI1 and block its interaction with RNA helicase A in Ewing's sarcoma [99]. It was later found that YK-4-279 also inhibited transcriptional activity of ERG and ETV1, but mechanism of action underlying this activity is not clear [100].

A collaboration among French and American scientists have identified DB1255 as an ERG/DNA binding inhibitor in the DNA minor groove in 2012 **(Figure 1.9)** [101]. This compound specifically interacts with the same DNA and consequently decreases the transcription by diminishing the binding of ERG transcription factor with DNA. By ELISA-derived Protein/DNA binding inhibition assay, DB1255 at 5 μM was shown to inhibit protein/DNA complex formation by more than 90%. It appears that DB1255 targets the protein-

DNA interface of the ERG/DNA complex. As ETS DBD domain is highly conserved, it remains to be verified whether DB1255 inhibits other ETS members that contain the ETS DBD domain.

1.7. Objectives

Overall, accumulating evidences suggest that ERG could be a promising therapeutic target for PCa. My objective of this project is to identify chemical compounds as ERG inhibitors.

CHAPTER 2. MATERIALS AND METHODS

2.1. Strategies to identify ERG inhibitors and overall workflow

It is well-known that it is very difficult to identify chemical inhibitors for a transcriptional factor. Although the NMR structure of the ERG PNT domain is available, no functional binding site are available on this domain for the binding of chemical compounds. I therefore turned to the ERG DBD domain. When this project began, there was no experimental structure for ERG DBD domain (to note that the crystal structure of ERG is now available as PDB entry of 4irg). I firstly constructed a structural model of human ERG DBD by homology modeling using the crystal structure of FLI1 DBD as a template (PDB entry: 1fli). Secondly, our strategy was to scan the molecular surface of ERG and combine structural findings with known biochemical data to identify a putative binding site for the design of chemical inhibitors. Recently, Loughran *et al.* found that a missense mutation (S329P) in the mice Erg DBD does not affect the protein stability and the mutant has binding affinity with DNA similar to that of the wild type, but the mutation of S329P abolished Erg transcriptional activity [65]. I found residue 329 is on the molecular surface

opposite to the DNA-interacting surface and identified a cavity near residue 329 (referred to as Site 2).

Since residue 329 is critical to the Erg transcriptional function, we reasoned site 2 could be a putative binding site for ERG inhibitors. Next, I have performed virtual screening against the three-dimensional NCI chemical database and our in-house database based on site 2 of the ERG DBD. Top-ranking candidates were first verified by ERG-dependent luciferase reporter assays. Hits were further evaluated a series of in vitro assays, including surface plasmon resonance analysis, Western blot, invasion assays and MTT assays. The overall workflow is illustrated in **Figure 2.1**.

2.2. Structural model of ERG DNA-binding domain and virtual screening

The ERG homology model was constructed using the Modeller software as implemented in Discovery Studio 2.5. Virtual screening was performed using software Gold against 50,000 compounds from the NCI chemical database and an in-house chemical database which include about 1000 compounds that were synthesized by our laboratory. Each Ser, Thr and Tyr OH was allowed to rotate to optimize hydrogen-bonding to the ligand, whereas other parts of the protein were kept rigid. Compounds were ranked according to Goldscore.

2.3. Chemicals and plasmids

The 39 top-ranked chemicals from the virtual screening were obtained from NCI. Compound **#648** was synthesized by our laboratory. Dimethyl sulfoxide (DMSO) of 0.7 % was

use as a solvent control. pMAX deltaN-ERG (Addgene, 29447), FLAG-ETS2 (Addgene, 28128) and pi-RES-puro-ELF3 (Addgene, 25728) were purchased from Addgene. The pCMV6-XL5-ETV1 was purchase from Origene (Catalog number: SC108403). Null was the internal control and purchased from Promega. pMSCV-ERG was kindly provided by Dr. Pandolfi, P., Harvard Medical School, Boston MA, U.S.A. pSG5-FLI1 was kindly provided by Dr. Trojanowska, M., Boston University, U.S.A. pTK-100-PUx3-Luc luciferase reporter was a kind gift from Dr. Oikawa, T., Tokyo, Japan. The plasmids were amplified by QIAGEN Plasmid Maxi Kit.

2.4. Cell lines

The human embryonic kidney HEK293 cells, and six prostate cancer cell lines, VCaP, LNCaP, 22Rv1, C4-2B, PC3 and DU145 were obtained from American Type Culture Collection (ATCC, Rockville, MD, USA) and maintained in DMEM (HEK293, VCaP) or RPMI-1640 (all others) supplemented with 10% fetal bovine serum (FBS) incubating with 5% CO_2 at 37^{o}C. VCaP cells are TMPRSS2-ERG positive, AR-positive and androgen dependent. LNCaP cells are AR-positive, express T877A mutated AR, androgen-dependent and are TMPRSS2-ETV1 positive [102]. 22Rv1 cells are AR-positive, express the H874Y mutated AR, and androgen-independent. C4-2B is an LNCaP variant isolated from castrated mice with preferential growth in bone. PC3 cells are AR negative, androgen independent prostate cancer and express ETV4 [103]. DU145 cells are AR-negative and androgen independent.

2.5. Transient transfection and luciferase reporter assay

HEK293 cells were seeded in 24-well plates with 1 x 10^5 of culture media and incubated for 24 hours. The cells were transfected using the calcium phosphate method with designated target plasmid, pTK-100-PUx3-Luc reporter and null as the internal control. Calcium phosphate transfection was involved the following two agents: 2X HBS, pH 7.05 (50 mM HEPES, 10 mM KCl, 12 mM Dextrose, 280 mM NaCl, 1.5 mM Na_2HPO_4) and 2.5 M $CaCl_2$. For the 24-well plate, HEK293 cells were at 70 – 80% confluence at the day of the transfection. Designated plasmids were mixed with 2.5M $CaCl_2$ solution (called Mixture 1). Then, the transfection complex was prepared with the same amount of volume of 2X HBS with the $CaCl_2$ solution, and was added dropwise while vortexing into Mixture 1. After 5 hours of transfection, the transfection complex was removed and then cells in phenol-red free DMEM medium with 10% charcoal-stripped FBS were exposed to DMSO vehicle control or compounds at designated concentrations. After further 24-hour, medium was removed and cells were harvested by 1x lysis buffer of 100 µL in each well (Promega dual-luciferase reporter assay kit, Canada). The harvested cells were stored in -80^{o}C prior to luciferase activity examination.

Luciferase activity was measured in 20 µL of sample using 50 µL luciferase assay reagent II to generate a "glow-type" luminescent signal, and thereafter adding 50 µL Stop & Glo ® reagent in the same tube to quench the reaction (Promega dual-luciferase reporter assay kit, Canada) in Promega Glomax 20/20 ^{TM} Luminometer.

Experiments were done in triplicate and were repeated at least 3 times. The relative luciferase unit (RLU) was calculated by dividing the firefly luciferase reporter by the *Renilla* luciferase internal control. The RLU units of vehicle control were normalized into 1. The fold of

suppression was calculated by dividing the fold of induction of the DMSO vehicle control by the fold of induction of the compound. The bigger the fold of suppression of the compound indicated the stronger inhibitory activity. The fold of suppression could still vary from one experiment to another experiment slightly, but this parameter was a good measurement for the potency and it was comparable among different experiments using the same protocol.

2.6. Surface plasmon resonance assay

Purified recombinant human ERG protein was purchased from Origene (Catalog number: TP308093). Similar to Rahim *et al.* [100], high-density ERG (6000 response units (RU)) and reference surfaces (no ERG) were amine-coupled to CM5 sensors using BIACORE 3000 instrumentation. To examine binding specificity, compounds (5 mM stocks in 80% DMSO / 20% water) were diluted to 50 μM (in HBS-EP running buffer containing 5% DMSO final concentration) and injected over reference and ERG-immobilized surfaces in tandem (25 μL/minute x 2 minutes association + 2 minutes dissociation). Between sample injections, surfaces were regenerated at 50 μL/minute using 30 second pulses of solution A (1M NaCl in running buffer) and solution B (0.05% Empigen in Pierce Gentle Elution buffer). To examine binding affinity, concentration series for **#648** and YK-4-279 (0, 10, 20, 30, 40, 50 μM) were titrated in the similar manner. SPR data were double-referenced and was representative of duplicate injections acquired from two independent trials.

2.7. Western blot analysis

Cell lines were plated in two wells of a 6-well plate at $0.5x10^6$ cells/mL incubated for 24 hours at 37°C, 5% CO_2. After allowing cells to attach, cells were harvested and homogenized in NP-40 lysis buffer (Sigma) containing a complete protease inhibitor cocktail (Roche). Forty micrograms of each protein extract were boiled in SDS sample buffer, size fractionated by 10% SDS-PAGE gels, and transferred onto a PVDF membrane (GE Healthcare). Next, blocking in 5% nonfat dry milk, membranes then were incubated with one of the following primary antibodies: anti-EZH2 mouse polyclonal (1:500, BD Biosciences, 612666), anti-ERG1/2/3 rabbit polyclonal (1:1000, Santa Cruz, C-17), anti-c-Myc rabbit polyclonal (1:500, Santa Cruz, N-262), anti-AR mouse monoclonal (1:1000, Santa Cruz, 441), anti-nucleoli mouse monoclonal (1:1000, Millipore, MAB1277), or anti-β-actin mouse monoclonal (1:5000, abcam, AC-15, ab6276). Following three washes in TBS-T, the blot was incubated with horseradish peroxidase conjugated secondary antibody and the signals visualized by enhanced chemiluminescence system as described by the manufacturer (GE Healthcare).

2.8. Boyden chamber invasion assay

Cell culture transwell inserts (24-well format, 8 µM pores, Falcon) were precoated with 2 µg Matrigel Basement Membrane Matrix (BD Biosciences). VCaP, LNCaP, and DU145 were plated at respectively 5×10^5, 1×10^5, and 1×10^4 cells/well in media with 0.5% FBS in transwells. Medium containing 20% serum was added to the lower chamber as chemoattractant, and cells were incubated for 48 hours (VCaP and DU145) and 24 hours (LNCaP) at 37°C, 5% CO_2. Invading cells on the lower surface of the transwell were fixed with 3.7% formaldehyde (Sigma, F8775) and stained with 0.5% crystal violet (Sigma, C3886).

2.9. MTT assay

Prostate cancer cells were plated in 96-well plate at 0.3-0.5 x10^4 cells/well and were incubated for 72 hours at 37°C, 5% CO_2. The number of viable cells was measured by methyl thiazolyl diphenyl tetrazolium bromide (MTT) assay. The OD values (OD570) were evaluated by BMG LabTech POLARstar OPTIMA microplate reader. Each experiment was at least in triplicate and repeated three times.

2.10. Statistical analysis

The students' t-test was used to test for statistical significance, using GraphPad Prism for Windows, v4.0 (Graphpad Software, San Diego, CA). A p-value less than 0.05 was considered statistically significant and represented by *. A p-value less than 0.001 was represented by **, and A p-value less than 0.0001 was represented by ***.

CHAPTER 3. RESULTS

3.1. Homology model of ERG DNA binding domain

Sequence alignment of the ERG DBD with the sequence from the NMR structure of the human FLI1 DBD (PDB entry: 1fli) revealed 91.9% identity between them **(Figure 3.1)**. A structural model of ERG DBD was built, using the structure of FLI1 DBD as a template. Importantly, based on the ERG DBD structural model, we have identified a binding cavity near the residue S329 (referred to as Site 2) **(Figure 3.2)**. Molecular surface of ERG DBD is shown in **Figure 3.3**, indicating that Site 2 is opposite to the protein-DNA interface of the ERG/DNA complex.

3.2. Discovery of novel ERG and ETV1 inhibitors by virtual screening

Using software GOLD (The Cambridge Cystallographic Data Cetre), our team has virtually screened 50,000 compounds from NCI-3 dimension database and our in-house database against the binding pocket (Site 2). Each Ser, Thr, and Tyr OH was allowed to rotate to optimize hydrogen-bonding to the ligand, whereas other parts of the protein were kept rigid. The compounds were ranked according to the GOLD scores. I have selected 39 top-scored compounds to perform luciferase assays. Chemical structures of the 39 top-scored compounds are shown in **Figure 3.4**.

3.2.1. Discovery of compounds V131 and V154 from the NCI chemical database

I have evaluated the 39 NCI compounds by ERG-dependent reporter assays in HEK293 cells **(Figure 3.5)**. Western blotting analysis indicated that HEK293 cells did not express detectable level of ERG. ERG-expressing plasmid MSCV-ERG, pTK-100-PUx3-luc reporter and Null internal control were transiently transfected into HEK293 cells. Cells were exposed to NCI compounds at 10 μM for 24 hours. My reporter assays of these compounds resulted in discovery of **V131** and **V154** as ERG inhibitors. **V131** dose-dependently suppressed ERG-dependent reporter activity, whereas **V154** showed only modest activity **(Figure 3.6)**. Further reporter assays using pCMV6-XL5-ETV1 plasmid, I found that **V154** significantly inhibited ETV1 transcriptional activity **(Figure 3.7)**. Western blot analysis indicated that **V131** and **V154** at 10 μM and 20 μM did not substantially affect expression of ERG protein in VCaP cells, which were exposed to compounds for 48 hours (results not shown). Their chemical structures are shown in **Figure 3.8**.

3.2.2. Discovery of compound #648 from the in-house chemical database

In the past few years, our laboratory has accumulated about 1,000 chemical compounds (referred to as in-house chemical database). The chemical structure is shown in **Figure 3.8**. Some of these compounds were from other project of this lab and some other compounds were synthesized with an aim to expanding the in-house chemical database (without any specific targets in mind). Based on Site 2 of the ERG DBD, we have performed *in silico* screening against this in-house chemical database and top-scored compounds were subjected to ERG-dependent reporter assay in HEK293 cells. This study leaded to discovery of **#648** as a novel ERG inhibitor **(Figure 3.9)**. We showed that **#648** dose-dependently suppressed transcriptional activity of the wild-type ERG as well as the N-terminally truncated ERG **(Figure 3.10)**.

3.3. Surface plasmon resonance analysis confirmed direct binding of compound #648 to the ERG protein

Recombinant ERG (Origene, TP308093) proteins were immobilized on CM5 chips by amine coupling and 50 μM of **#648** compounds at 50 μM, with a negative control (bicalutamide) and a positive control (YK-4-279) were injected the surface (25 μL/minute x 120 seconds association + 120 seconds dissociation) Bicalutamide (negative control) yielded non-significant signal responses similar to the DMSO/buffer blanks, whereas **#648** yielded specific, significant ERG binding responses **(Figure 3.11**, see top**)**. As an internal control to validate our SPR data, the 12 response unit (RU) binding response that we observed with the YK-4-279 standard **(Figure 3.11**, see bottom**)** correlated well with previous literature [100]. Possible direct binding of **V131** with ERG will be investigated by our further work.

3.4. #648 suppressed expression of ERG-regulated genes

We showed that **#648** potently suppressed ERG-dependent reporter activity in luciferase assays. To further confirm that **#648** inhibits transcriptional activity of ERG, we evaluated effect of **#648** on the expression ERG-regulated genes by Western blot analyses. VCaP cells were exposed to **#648** at 5 μM and 10 μM for 48 hours. Our Western blot analyses indicated that **#648** substantially suppressed expression of EZH2 and c-Myc, which are direct target genes of ERG **(Figure 3.12)**. Our study also revealed that **#648** potently upregulated expression of the tumor suppressor NKX3.1. Interestingly, **#648** also inhibited expression of ERG. In addition, our western blot analysis indicated that **V131** at 10 μM did not substantially inhibit the expression of EZH2 and c-Myc in VCaP cells, which were exposed to 10 μM of **V131** for 48 hours (results not shown).

3.5. V131 and #648 inhibited ERG, FLI1, and ETS2 but not ELF3

In addition to ERG, ETV1 and N-terminally truncated ERG (dN-ERG), we have also evaluated **V131**, **V154** and **#648** against ETS2, FLI1 and ELF3 by reporter assays **(Figures 3.13−3.15)**. The fold of suppressions of our compounds against ERG, dN-ERG, ETV1, ETS2, FLI1 and ELF3 were summarized in **Table 1**.

As shown in **Table 1**, **V131**, **V154** and **#648** at 10 μM potently inhibited transcriptional activity of ERG. However, these compounds showed selectivity against other ETS factors. **V131** was active against ETS2 and FLI1, but inactive against dN-ERG, ETV1 and ELF3. **V154** at 10 μM potently inhibited ETV1 and is modestly active against ELF3, but was inactive against ETS2

(Table 1). Compound **#648** at 10 μM substantially inhibited ERG, ETS2 and FLI1, and modestly inhibited dN-ERG, but was inactive against ELF3.

Table 1. A summary of the fold of suppression of V131, V154 and #648 at 10 μM against selected members of ETS transcriptional factors in reporter assays.

	V131	**V154**	**#648**
ERG	**5.4**	**2.1**	**5.8**
dN-ERG	1.2	N.D.	1.6
ETV1	0.8	**2.6**	N.D.
ETS2	**1.7**	1.2	**1.8**
ELF3	0.6	1.6	0.7
FLI1	**1.9**	N.D.	**2.3**

Note: N.D, not determined.

3.6. V131 and #648 reduced invasion ability of VCaP cells, but not in DU145

Our Western blot analysis confirmed the previous finding that VCaP cells express substantial level of ERG protein, whereas LNCaP, C4-2B, 22Rv1, PC3 and DU145 cells did not express detectable level of ERG **(Figure 3.16)**. The analysis also confirmed that VCaP, LNCaP, C4-2B and 22Rv1 are AR positive, whereas PC3 and DU145 were AR negative (Figure 3.16). By Boyden chamber assay, we demonstrated that **V131 at 10** μM inhibited invasion in VCaP cells by ~80% when compared to the DMSO vehicle control, whereas **V131** at 10 μM had no

effect on invasion of DU145 cells **(Figure 3.17)**. Compound **#648** at 10 μM potently suppressed invasion of VCaP cells and had no effect on invasion of DU145 cells **(Figure 3.18)**. These results indicated that **V131** and **#648** selectively inhibited invasion of ERG positive PCa cells.

ETV1 directs androgen metabolism and confers aggressive prostate cancer in mice and patients [104]. LNCaP cells endogenously express ETV1. By Boyden chamber invasion assay, compound **V154** at 10 μM substantially inhibited invasion of LNCaP cells when compared to the DMSO vehicle control **(Figure 3.19)**. This was consistent with our finding from reporter assays that V154 at 10 μM significantly inhibited transcriptional activity of ETV1.

3.7. Cytotoxicity of compounds V131, V154, and #648 against VCaP, LNCaP, and DU145 cells

To evaluate cytotoxicity of **V131**, **V154**, and **#648** in VCaP, LNCaP and DU145 cell lines, cells were exposed to compounds at designated concentrations for 3 days and the number of viable cells were evaluated by MTT assays. Compound **V131** at a dose up to 40 μM showed no significantly cytotoxicity against VCaP cells. Compound **#648** at 10 μM was not cytotoxic to VCaP cells, but at 40 μM **#648** showed significant cytotoxicity against VCaP cells **(Figure 3.20)**. **V131** at 40 μM and **#648** at 10 μM were not cytotoxic to DU145 cells, but **#648** at 20 and 40 μM showed dose-dependent cytotoxicity against DU145 cells **(Figure 3.21)**.

V154 showed weak cytotoxicity against LNCaP cells. When LNCaP cells were exposed to **V154** at 20 μM for 3 days, there were ~80% viable cells, whereas exposure to **V154** at 40 μM for 3 days resulted in 60% viable cells when compared with DMSO vehicle control. In contrast, **V154** at doses up to 40 μM showed no cytotoxicity against DU145 cells **(Figure 3.22)**.

CHAPTER 4. DISCUSSION

4.1. #648 as a novel ERG inhibitor

Compound **#648** was identified as a novel ERG inhibitor. **#648** at 5 and 10 μM substantially inhibited the invasion of VCaP cells (ERG positive) **(Figure 3.18)**. Such activity was not due to the toxicity as my MTT assay revealed that **#648** at 10 μM was not cytotoxic to VCaP cells **(Figure 3.20)**. By Western blot analysis, we showed that **#648** significantly suppressed expression of ERG, EZH2 and c-Myc in VCaP cells **(Figure 3.12)**. As EZH2 is a driver of metastasis [105], the inhibition of VCaP cells invasion by **#648** could be at least in part mediated by inhibition of EZH2 expression. c-Myc is a oncogenic transcription factor and is one the most frequently activated oncogenes in many human cancers with various influence on cell proliferation and survival. A recent study has shown c-Myc acts a downstream effector of AR to reinforce androgen signaling [106] and overexpression of ERG was positively correlated to the overexpression c-Myc [68]. In addition, Mani *et al.* found upregulation of TMPRSS2–ERG resulted in the concomitant upregulation of wild-type ERG transcription in VCaP cells, suggesting dN-ERG protein may upregulate expression of wild-type ERG by a feed-forward mechanism [107]. Therefore, inhibitory activity of **#648** against dN-ERG (**Figure 3.10)** could suppress expression of ERG protein in VCaP cells **(Figure 3.12)**.

Our SPR analysis indicated that **#648** inhibited ERG through direct binding with ERG protein. However, further work is required to verify whether **#648** binds with ERG at Site 2, which is near the residue S329 **(Figure 3.3)**. Further studies on molecular mechanisms of action of **#648, V131** and **V154** are needed. It has been found that PARP1 and DNA-PKcs are coactivators of the ERG transcriptional activation [108]. It remains to be verified whether **#648**

and **V131** disrupts association of ERG with its coactivators. Furthermore, our team will design and synthesize a series of derivatives of our lead compounds **V131**, **V154** and **#648** to optimize the bioactivities.

4.2. V131 as a novel ERG inhibitor

V131 was also identified as a novel ERG inhibitor. **V131** at 5 and 10 μM inhibited the invasion of VCaP cells (ERG positive) **(Figure 3.17)**. Such activity was not due to the toxicity since my MTT assay revealed that **V131** at 10 μM was not cytotoxic to VCaP cells **(Figure 3.20)**. In the Western blot analysis, **V131** at 20 μM did not have a substantial effect on the expression of ERG, EZH2 and c-Myc in VCaP cells (results not shown). The limitation of my experiment design was there might be other target genes associated with invasion and metastasis, such as MMP3 and MMP9, which I have not investigated. Further work should investigate the effect of **V131** on MMP3 and MMP9 expression by Western blot analyses.

In addition, in my reporter assays, I have obtained a wide range of fold of induction, ranging from 2 folds to 50 folds for plasmids expressing different members of ETS factors. First of all, these plasmids are not in the same vectors. The low folds of induction (below 5 folds) for the results of pMSCV-ERG **(Figure 3.6** & **3.9)**, pMAX dN-ERG **(Figure 3.10)** and pSG-FLI1 **(Figure 3.14)** might be due to low transfection efficiency. Therefore, I propose to clone the cDNA into pcDNA 3.1 expression vector since pcDNA3.1-ETS2 has produced ~50 folds of induction in the DMSO control **(Figure 3.13)**. I also propose to include more low concentration doses in MTT assays so that I can know clearer how low the toxicity of **V131** in the cell lines. SPR analysis will be done to confirm whether **V131** has direct binding to ERG or not.

4.3. V154 as a novel ETV1 inhibitor

V154 was identified as a novel ETV1 inhibitor. **V154** at 5 and 10 μM inhibited the invasion of LNCaP cells (ETV1 positive) **(Figure 3.19)**. Such activity was not due to the toxicity as my MTT assay revealed that **V154** at 10 μM was not cytotoxic to LNCaP cells **(Figure 3.22)**. Chromosomal rearrangements involving TMPRSS2-ETV1 can result in the overexpression of ETV1 [37]. ETV1 mRNA and protein are up-regulated in response to ligand-activated AR in androgen-dependent LNCaP cells, which endogenously express TMPRSS2-ETV1 fusion gene [109].

My preliminary data will need more experiments to be further strengthened. I will need a negative control experiment in ETV1-negative, such as DU145 cells so that I have stronger evidence that **V154** has selectivity in both luciferase assay and invasion assay targeting ETV1. ETV1 protein expression will be examined after the treatment of **V154** in LNCaP cells. I propose SPR analysis to confirm possible direct binding to ETV1 protein.

.

4.4. The challenge of discovery of ERG inhibitors

Transcription factors are historically considered to be “undruggable” [110]. Although the NMR structure of the ERG PNT domain is available, no functional binding site are available on this domain for the binding of chemical compounds. A key step in target-based virtual screening is to identify a binding site on the 3D structure. We have successfully identified **V131**, **V154** and **#648** as ERG inhibitors based on virtual screening study. Inspired by the recent finding that S329P mutation resulted in loss of transcriptional activity of Erg, I have boldly hypothesized that

Site 2 near reside S329 could be a binding site for ERG inhibitors (**Figure 3.3)**. However, it remains to be verified whether compounds **V131**, **V154** and **#648** bind ERG at Site 2.

4.5. Clinical implications

To develop AR inhibitors that are capable of effectively suppressing the sustained AR signaling in CRPC cells has been challenging in the field. Metastatic disease presents a continuing therapeutic challenge and is the most common cause of cancer-related death [111]. As recent studies indicated that localized PCa with TMPRSS2-ERG positive is prone to lymph node metastasis, ERG inhibitor could potentially prevent patients with localized PCa from progression to metastatic PCa.

FIGURES LIST

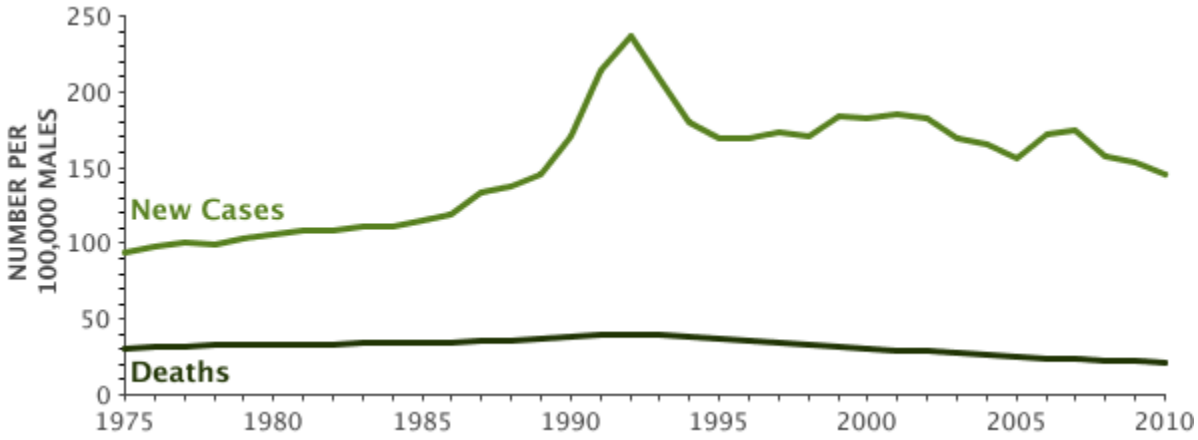

Figure 1.1. Prostate cancer incidence and mortality in USA from 1975 to 2010 [37].

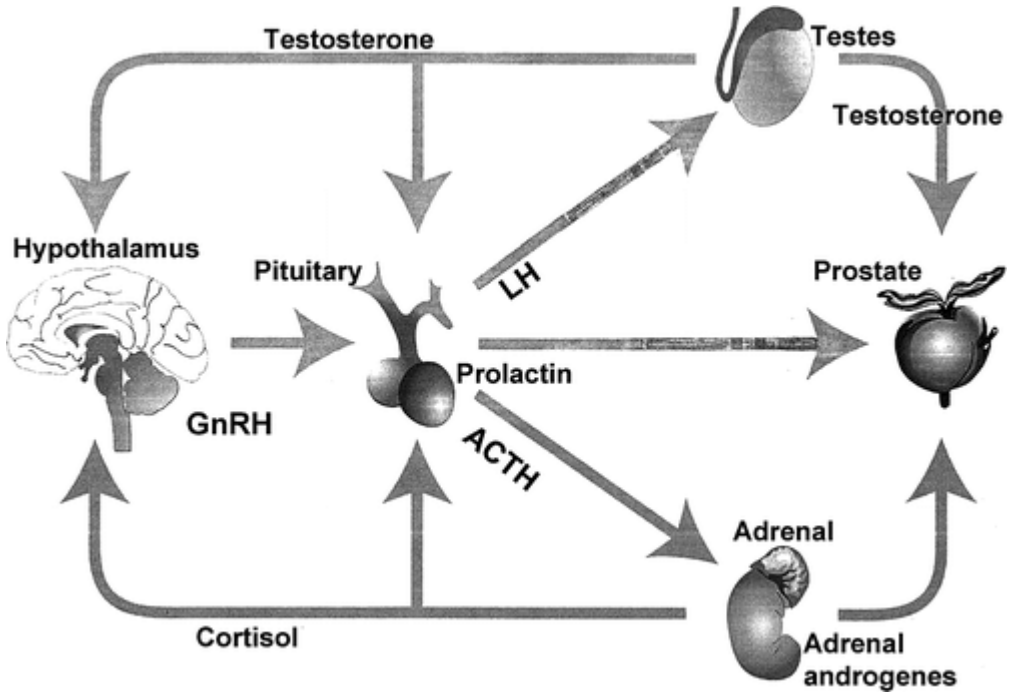

Figure 1.2. The endocrine control of the prostate gland. The main regulator is testosterone, which is produced from the testes (95%) and the adrenals (5%). Testosterone production is regulated by LH (testes) and ACTH (adrenals). The pituitary production of LH is regulated by GnRH from the hypothalamus [129]. Abbreviations: GnRH, gonadotropin-releasing hormone ; LH, luteinizing hormone; ACTH, adrenocorticotropic hormone

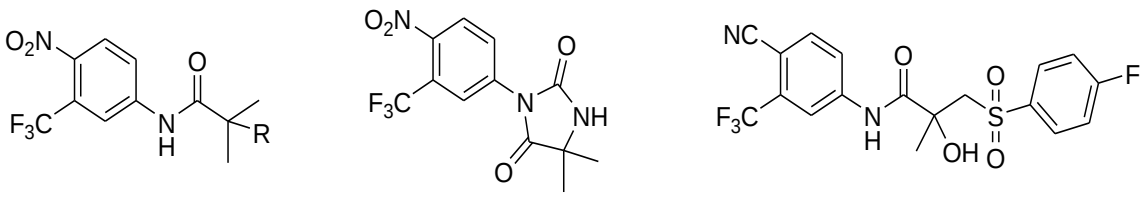

Flutamide (R=H)
Hydroxyflutamide (R=OH)

Nilutamide

Bicalutamide

Figure 1.3. Nonsteroidal antiandrogens are currently used in the clinic.

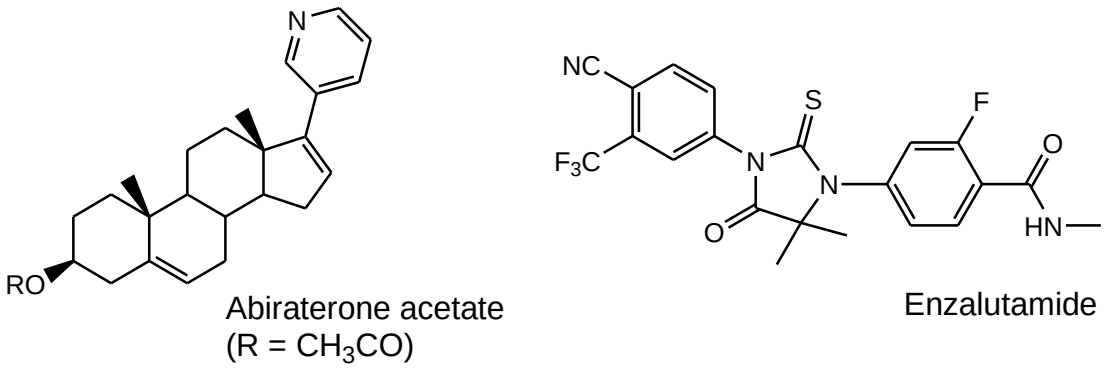

Figure 1.4. Abiraterone acetate and enzalutamide have been recently approved by FDA for CRPC patients.

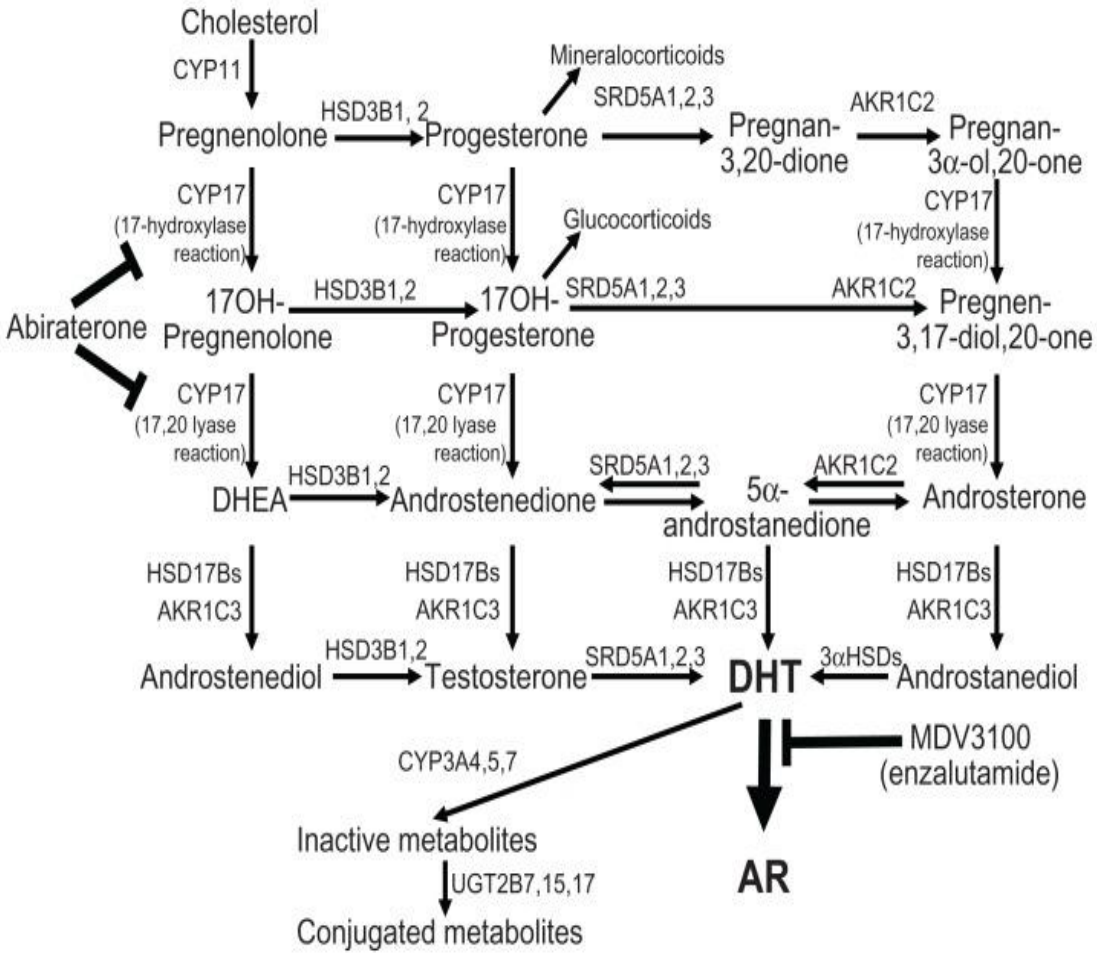

Figure 1.5. Enzymatic pathways of androgen synthesis, and target sites of recent approved drugs. Abiraterone is a CYP17 inhibitor and enzalutamide (or previously referred as MDV3100) is an antagonist of AR [45].

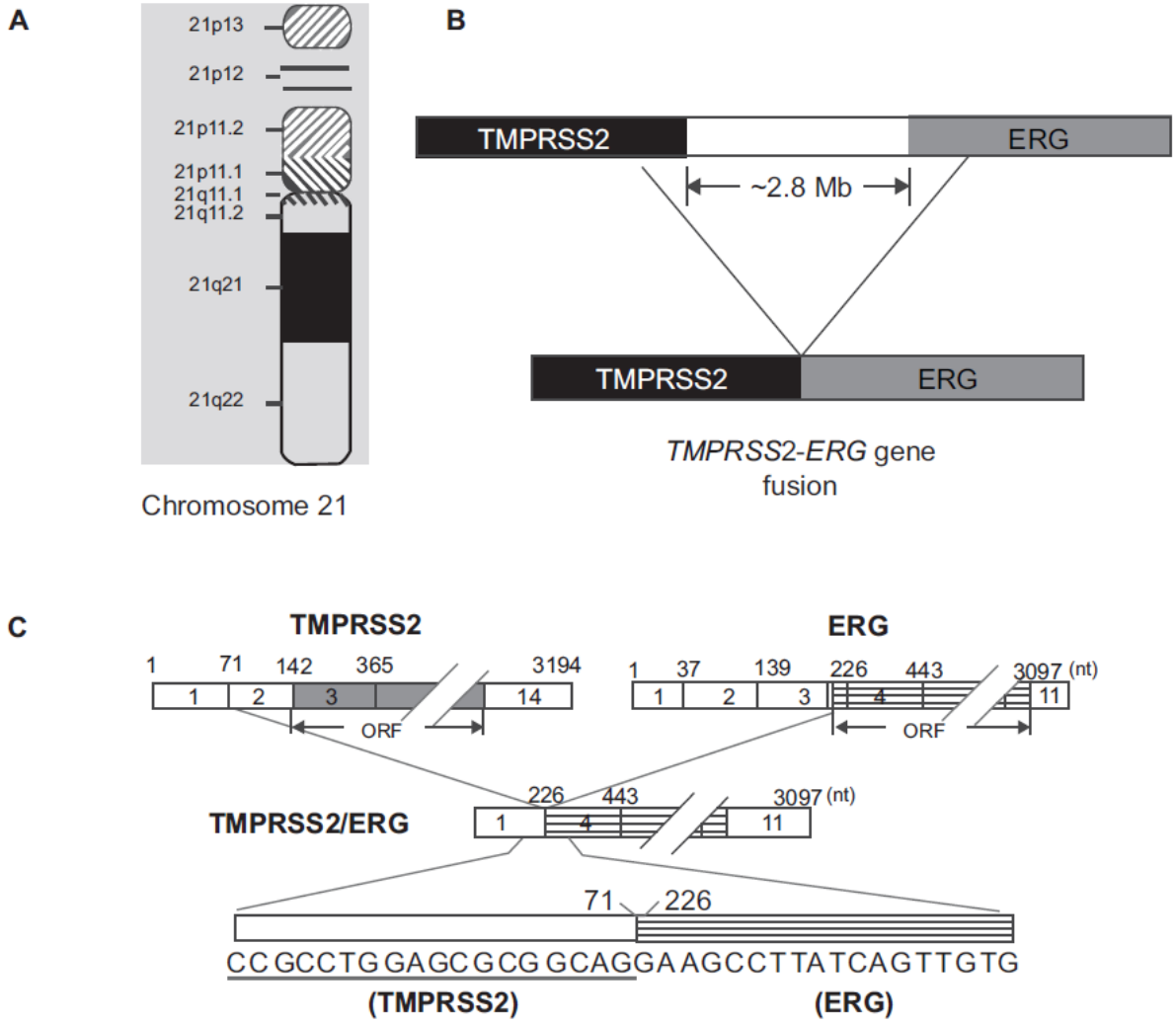

Figure 1.6. TMPRSS2-ERG fusion gene. A) Ideogram of chromosomal 21. B) Interstitial deletion and formation of the TMPRSS2-ERG fusion. C) Schematic illustration of the exons and gene sequences in the TMPRSS2-ERG gene fusion. The grey box represents the open reading frame (ORF) of TMPRSS2 while the striped box represents the open reading frame of ERG. Each exon is indicated by numbers in the boxes and the numbers above the boxes are the last base of each exon. Sequences at the fusion junction are indicated and the sequence from TMPRSS2 is underlined [131].

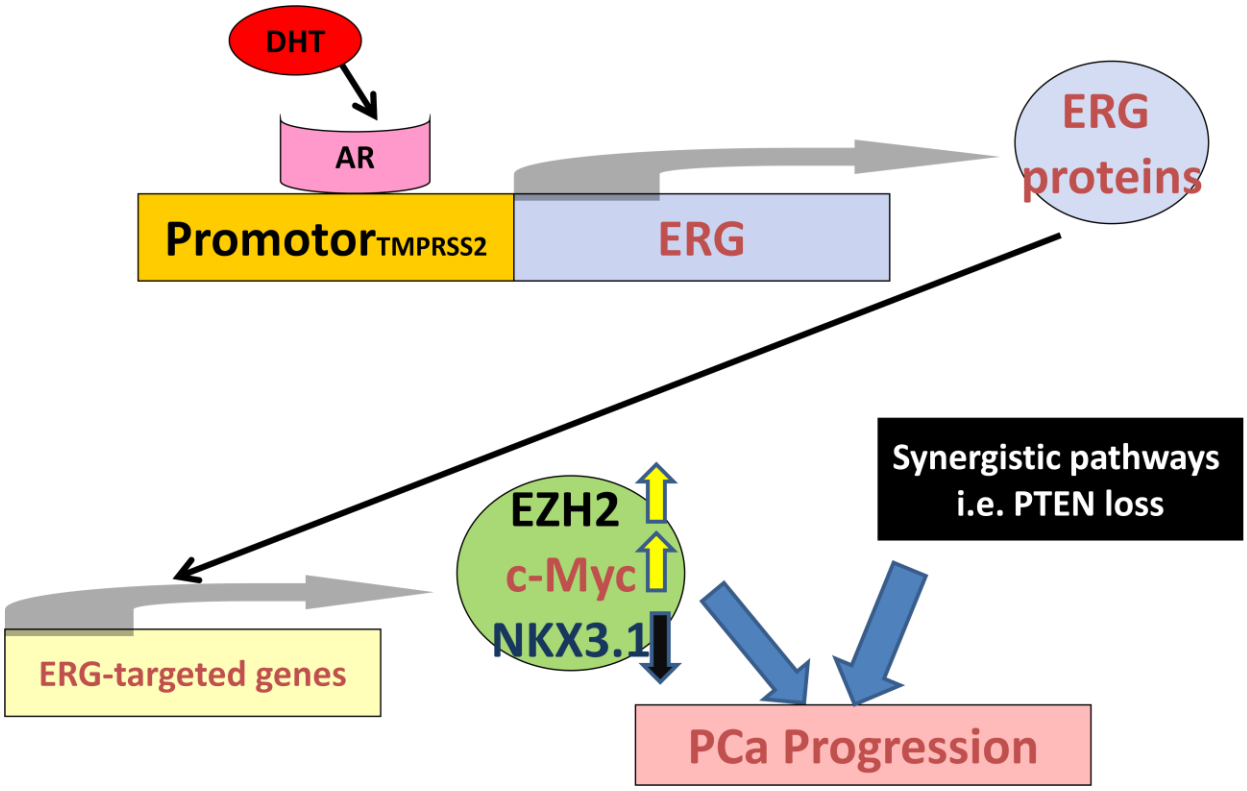

Figure 1.7. Possible roles of TMPRSS2-ERG fusion gene in prostate cancer progression. The protein product of TMPRSS2-ERG fusion is the ERG protein. The ERG upregulates expression of EZH2. ERG also upregulates c-Myc oncogene and down-regulates tumor suppressor NKX3.1.

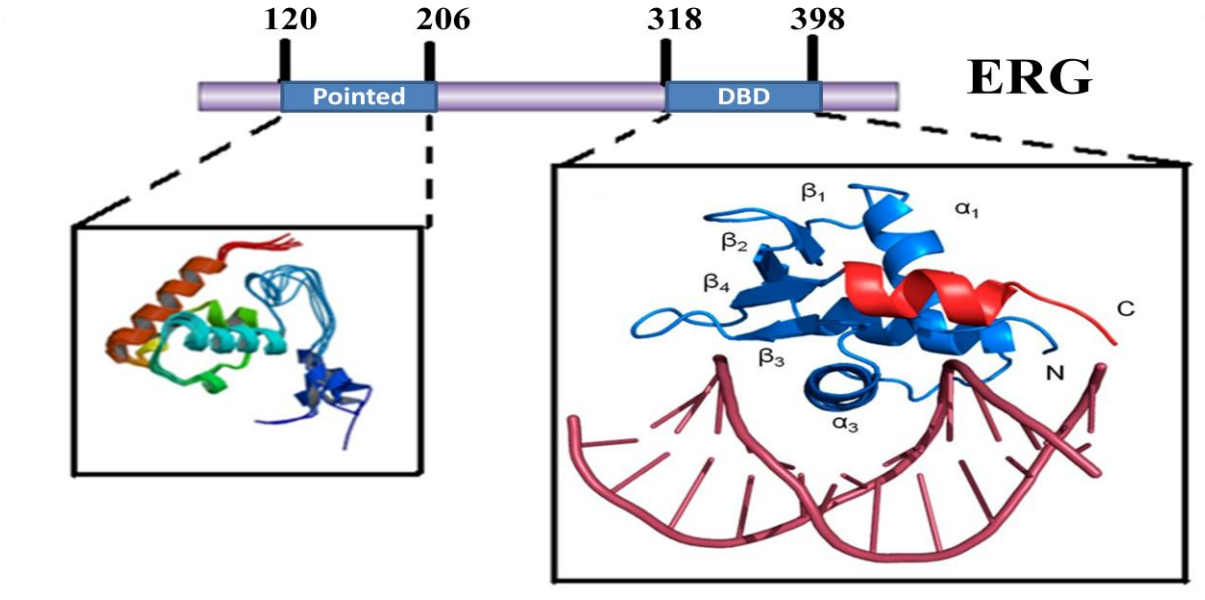

Figure 1.8. ERG pointed domain, DNA binding domain, and their 3D structural protein models. Pointed domain (PBD entry of pointed domain: 1sxe). The crystal structure of ERG DBD was not available until January 2013 (PBD entry: 4irg).

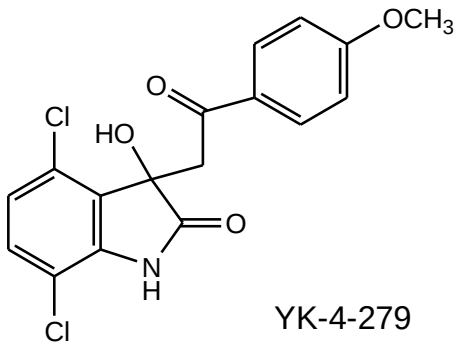

YK-4-279

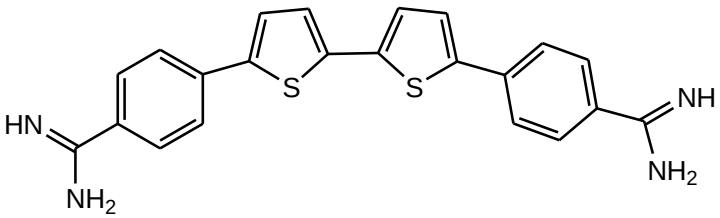

DB1255

Figure 1.9. The chemical structure of YK-4-279 and DB1255 are ERG inhibitors.

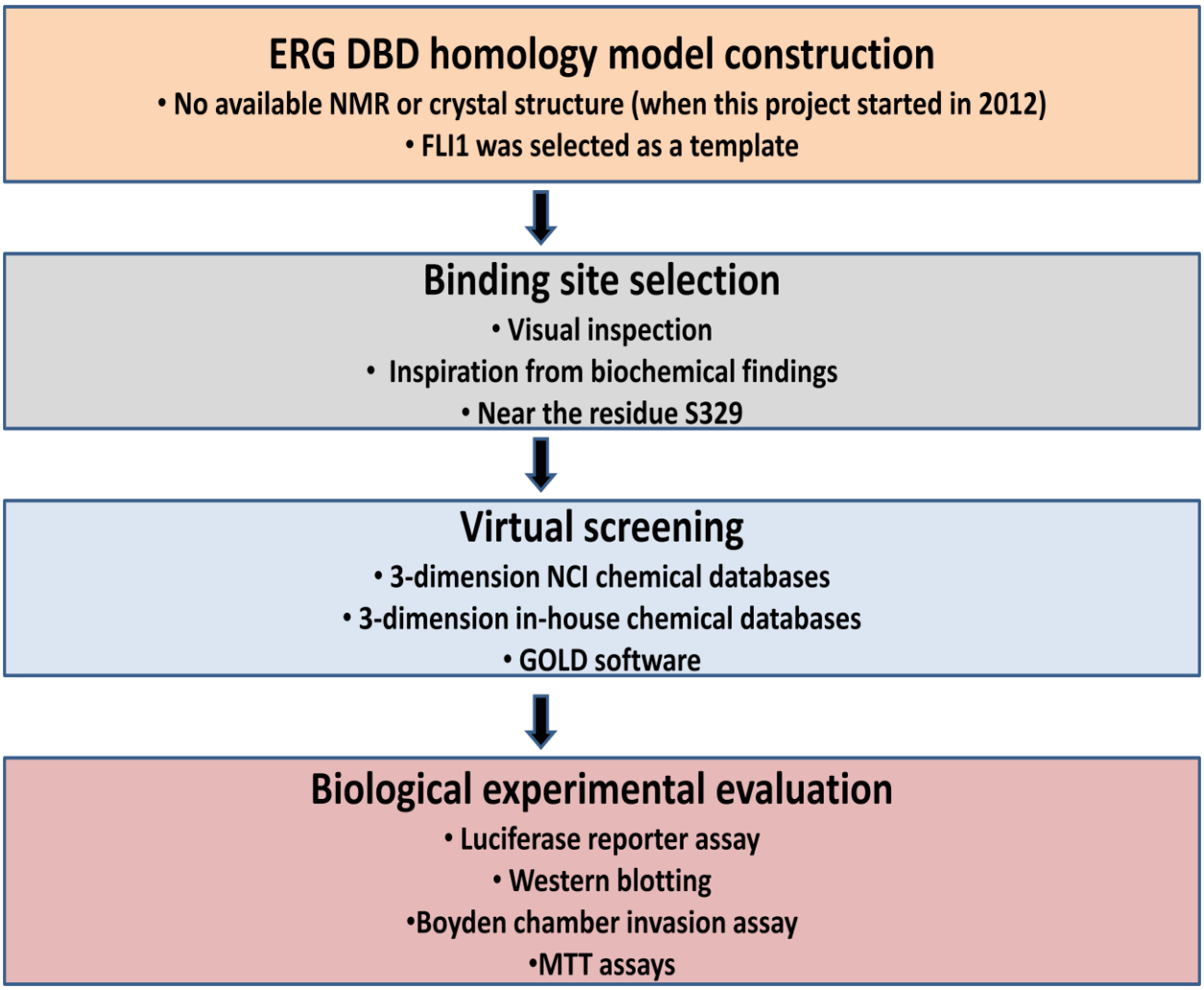

Figure 2.1. A workflow from the dry lab to the wet lab for discovery of ERG inhibitors.

Figure 3.1. ERG and FLI1 amino acid sequence alignments (91.9% identity).

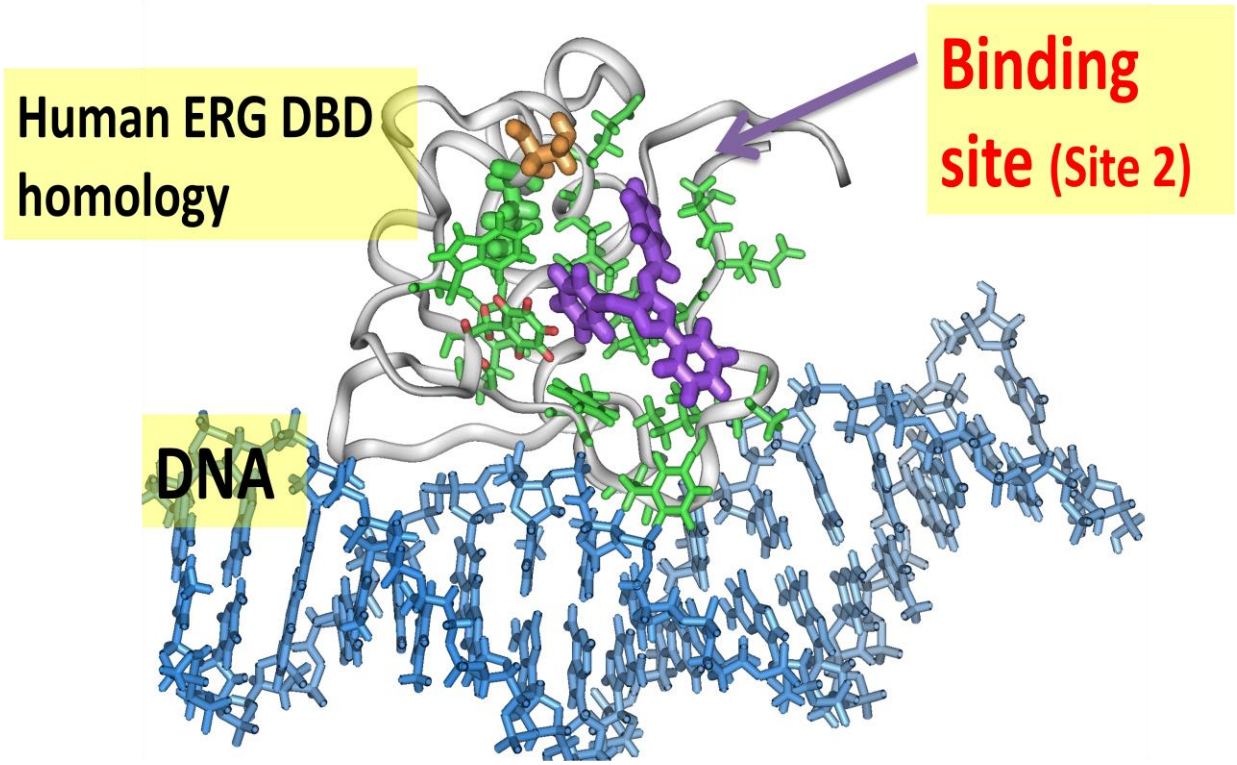

Figure 3.2. Human ERG DBD homology model. The DBD is shown in white ribbon. DNA is in sticks (in blue). The identification of a possible binding site (referred to as Site 2) is inspired by biochemical data involving Erg residue S329 [82]. A compound (in purple) is docked on the binding site (in green). Residue S329 is shown (in orange).

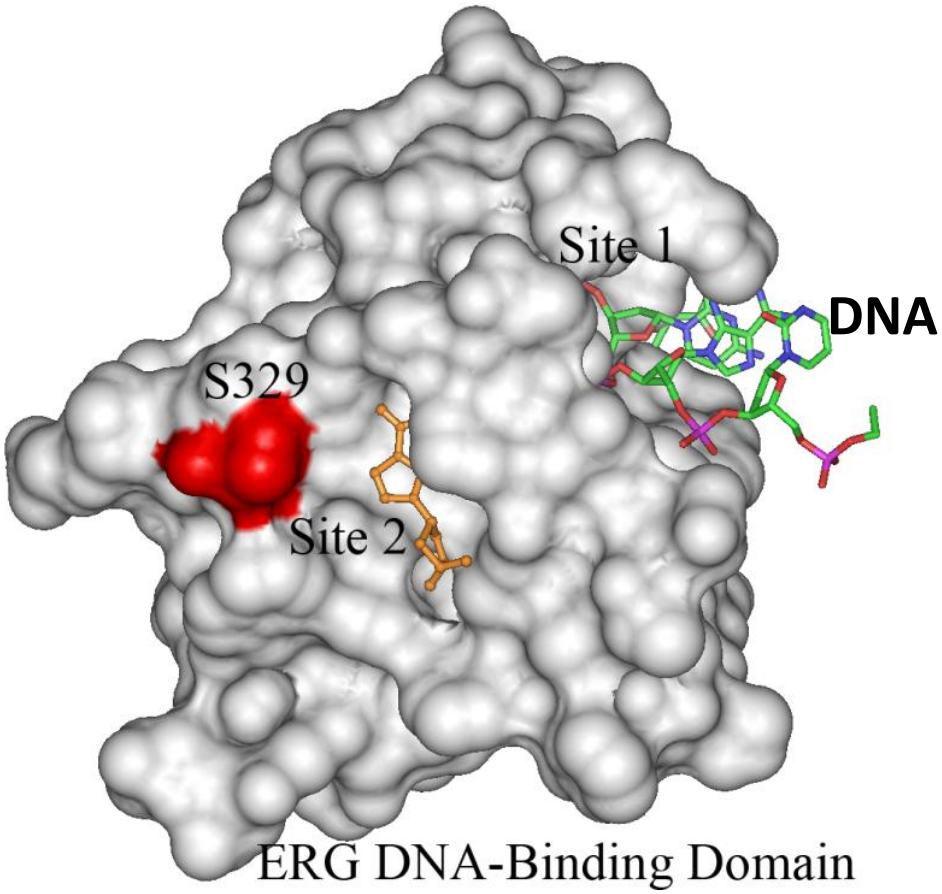

Figure 3.3. Molecular surface of ERG DBD. DNA is in sticks and is colored according to the atomic-coloring scheme (C in green, N in blue, O in red and P in pink). Binding site 1 interacts with DNA. Molecular surface of residue S329 is in red. We discovered there is a binding site (Site 2) near residue 329. A compound (in orange sticks) is docked into Site 2.

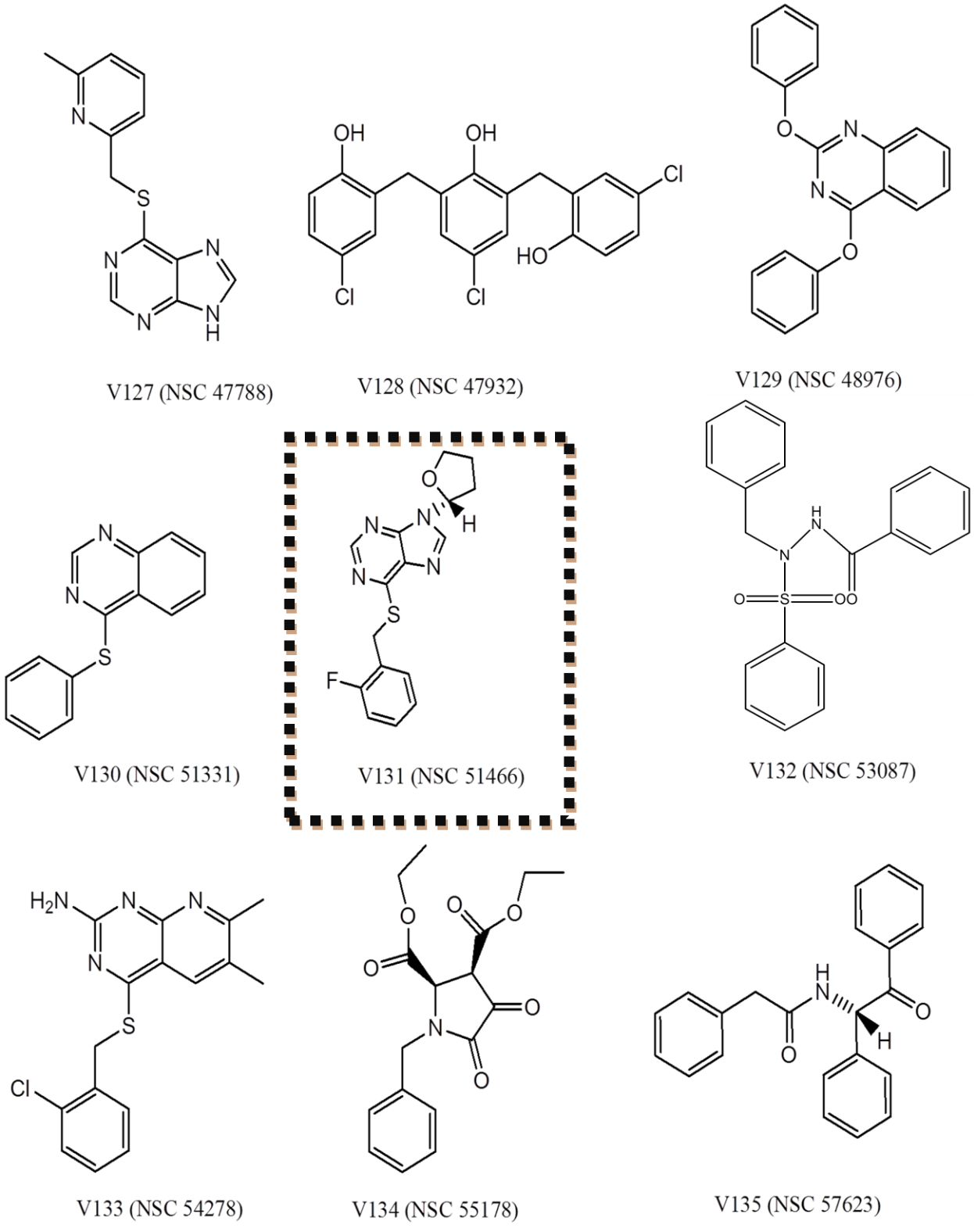

Figure 3.4. Chemical structures of 39 top-scored NCI compounds. (continued)

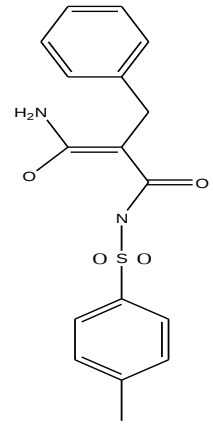

V136 (NSC 60177)

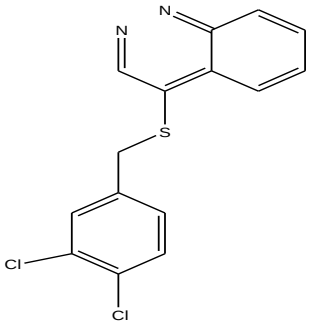

V137 (NSC 62411)

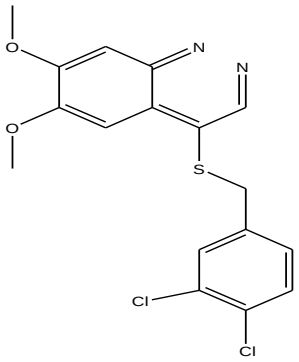

V138 (NSC 64814)

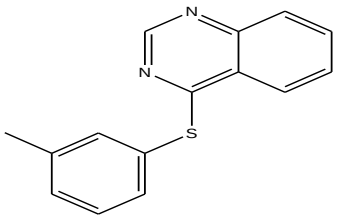

V139 (NSC 65059)

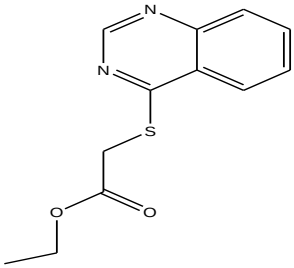

V140 (NSC 65061)

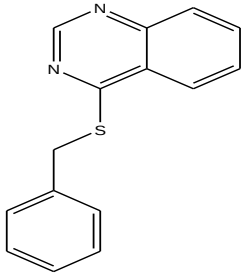

V141 (NSC 65066)

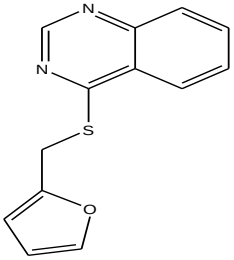

V142 (NSC 65068)

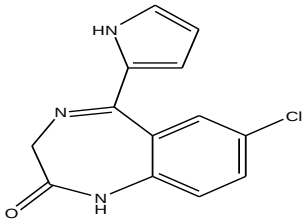

V143 (NSC 66020)

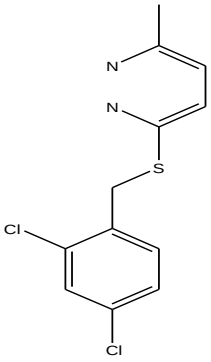

V144 (NSC 66081)

Figure 3.4. Chemical structures of 39 top-scored NCI compounds. (continued)

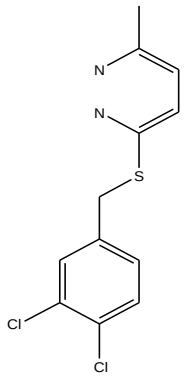

V145 (NSC 66082)

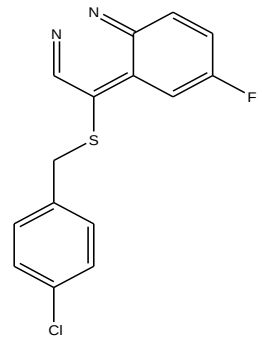

V146 (NSC 66094)

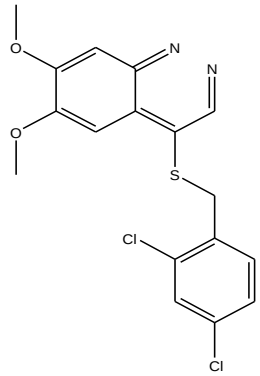

V147 (NSC 66107)

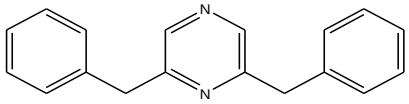

V148 (NSC 165503)

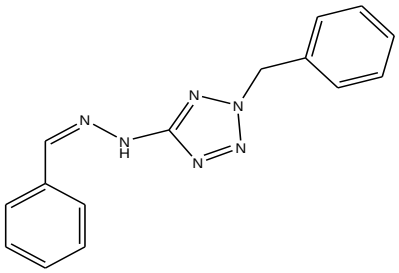

V149 (NSC 168225)

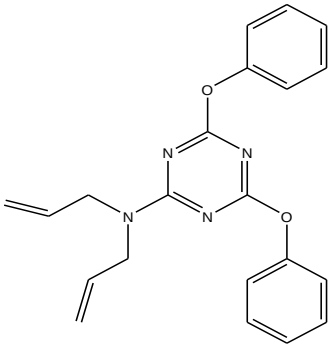

V150 (NSC 170041)

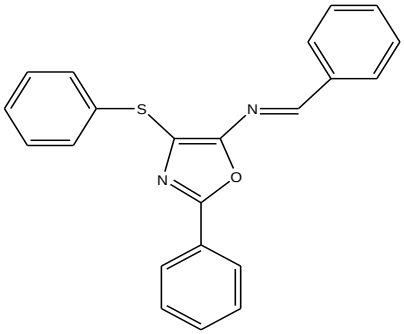

V151 (NSC 177918)

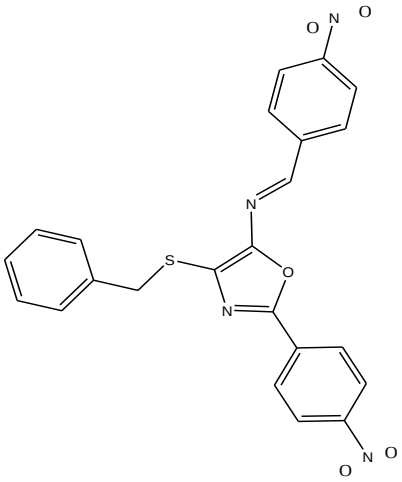

V152 (NSC 177922)

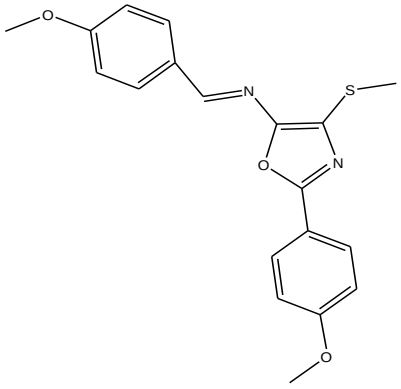

V153 (NSC 177923)

Figure 3.4. Chemical structures of 39 top-scored NCI compounds. (continued)

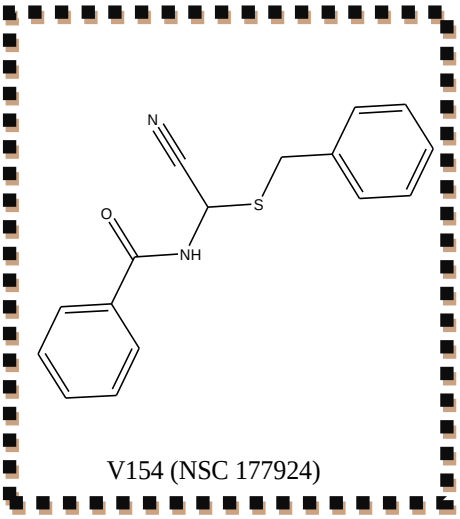

V154 (NSC 177924)

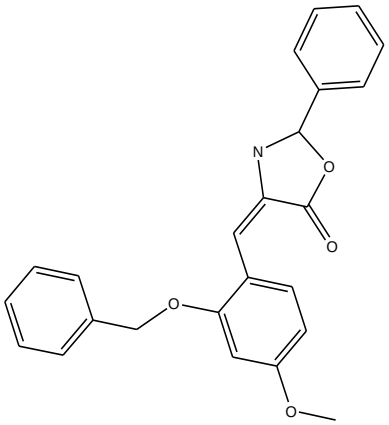

V155 (NSC 262665)

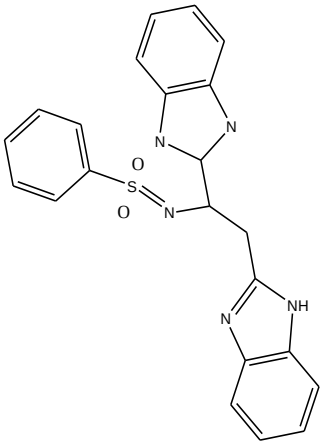

V156 (NSC 283787)

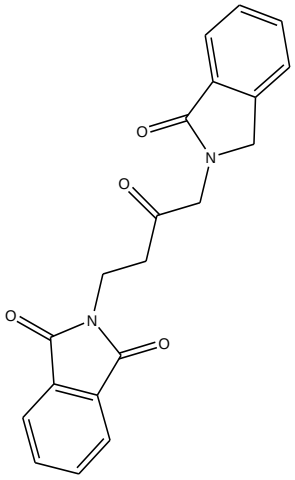

V157 (NSC 351351)

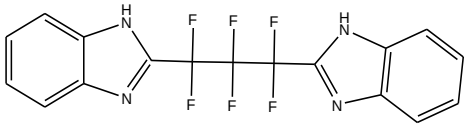

V158 (NSC 353884)

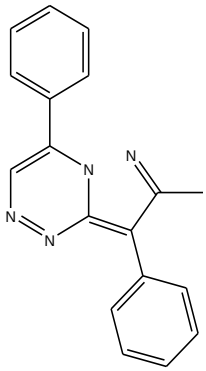

V159 (NSC 355166)

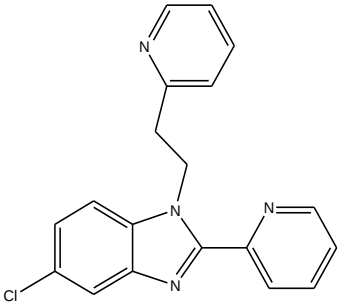

V160 (NSC 356785)

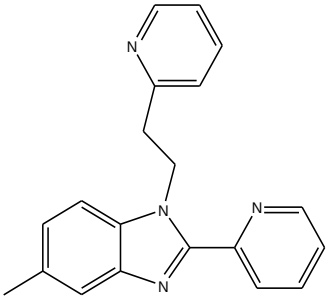

V161 (NSC 356790)

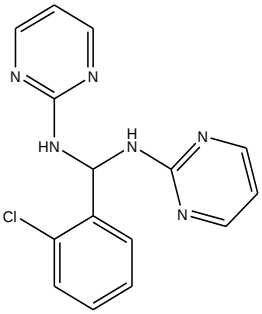

V162 (NSC 357650)

Figure 3.4. Chemical structures of 39 top-scored NCI compounds. (continued)

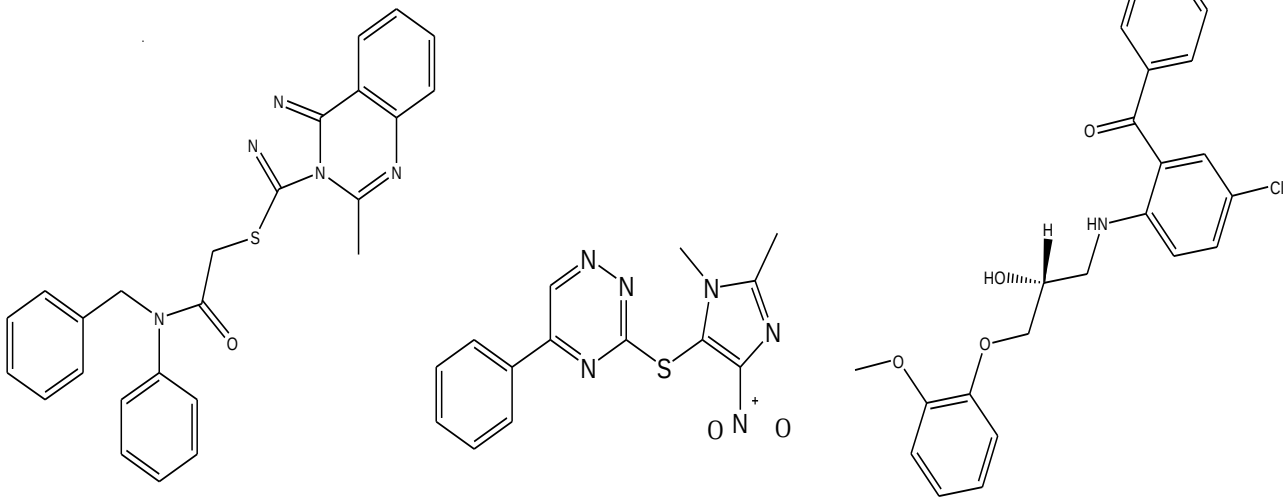

V163 (NSC 357689)

V164 (NSC 359685)

V165 (NSC366098)

Figure 3.4. Chemical structures of 39 top-scored NCI compounds.

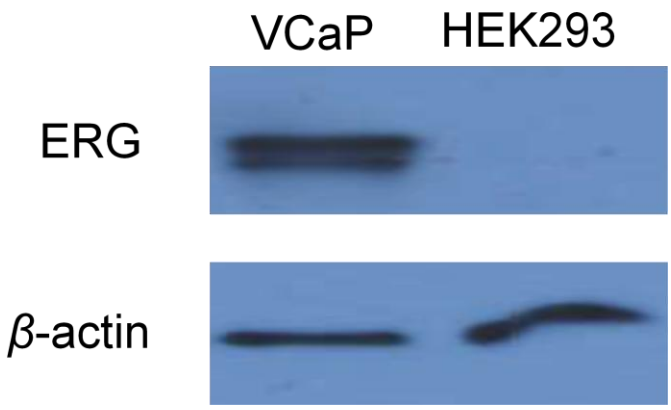

Figure 3.5. Endogenous expression of ERG in VCaP but not in HEK293 cells. VCaP is a prostate cancer cell line which is TMPRSS2-ERG positive but the human embryonic kidney HEK293 cells are not.

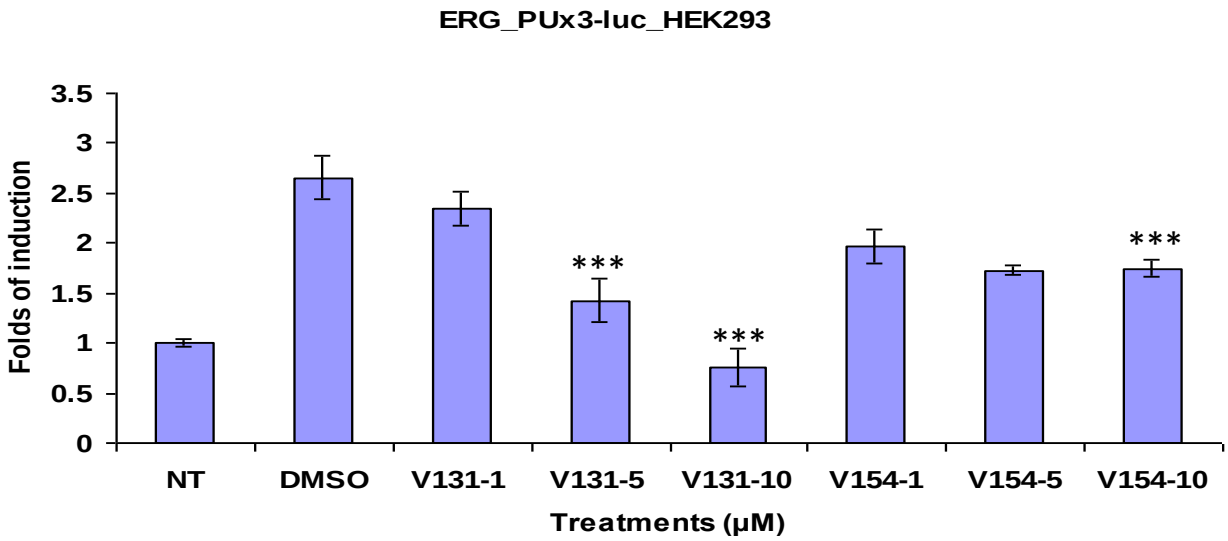

Figure 3.6. V131 and V154 dose-dependently suppressed ERG-dependent luciferase activity in HEK293 cells. pMSCV-ERG, pTK-100-PUx3-Luc luciferase reporter, and Null (internal control) were transfected into HEK293 cells using calcium phosphate method. NT (internal control) was transfected with empty vector pMSCV, pTK-100-PUx3-Luc and Null, and treated with DMSO. Cells were exposed to treatments for 24 hours. The experiment was repeated three times in triplicate. *** p-value < 0.0001 when compared with DMSO vehicle control.

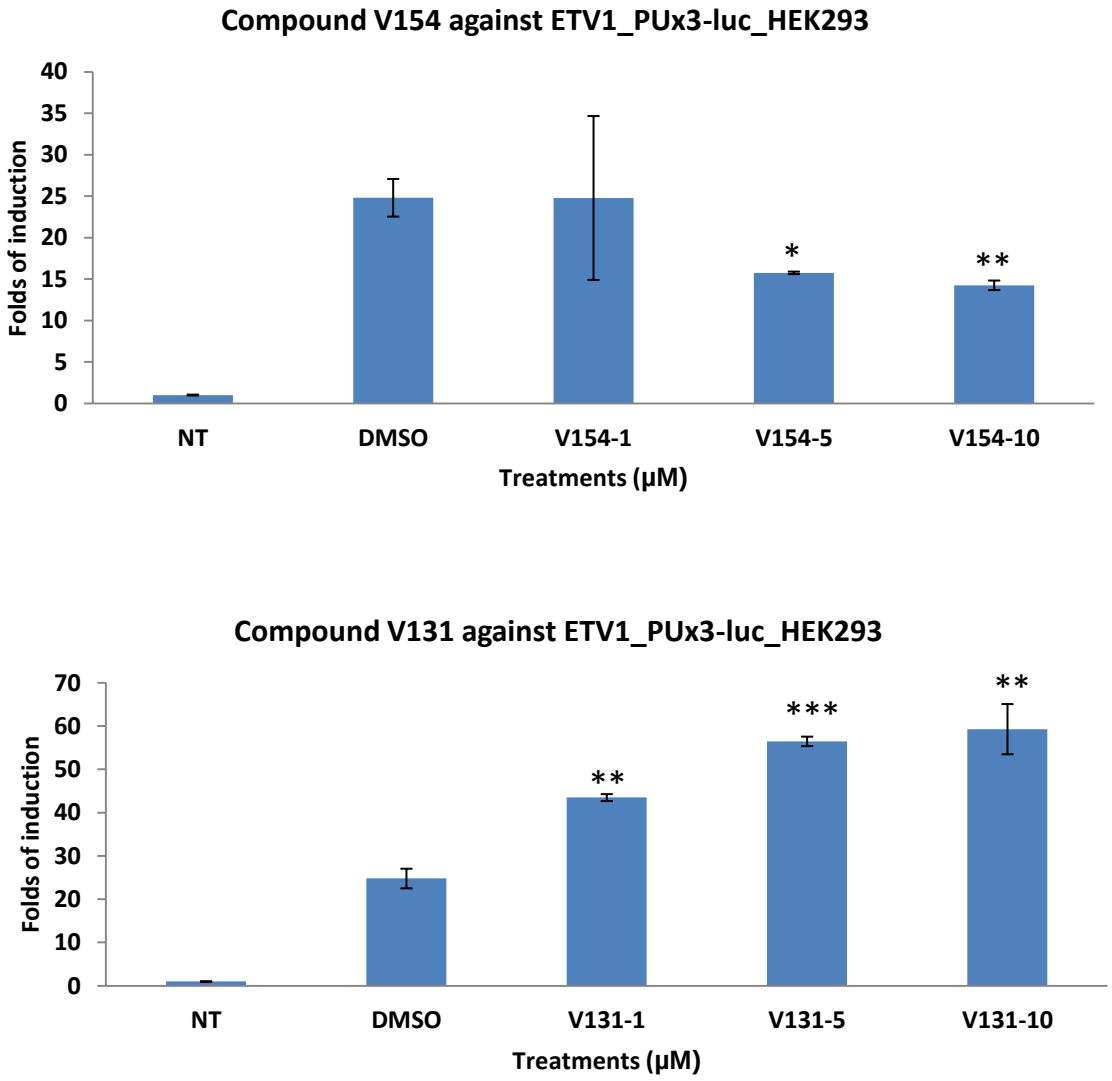

Figure 3.7. V154 dose-dependently suppressed ETV1-dependent luciferase activity in HEK293 but V131 promoted ETV1 luciferase activity. pCMV6-XL5-ETV1, pTK-100-PUx3-Luc luciferase reporter, and Null were transfected into HEK293 cells using calcium phosphate method. NT (internal control) was transfected with empty vector pCMV2, pTK-100-PUx3-Luc and Null, and treated with DMSO. The experiment was repeated three times. The experiment was repeated three times in triplicate. ** p-value < 0.001 or *** p-value < 0.0001 when compared with DMSO vehicle control.

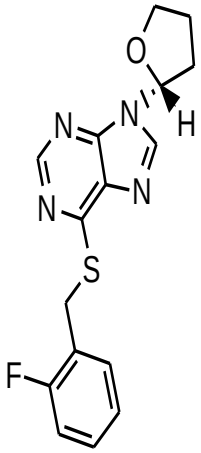

V131 (NSC 51466)

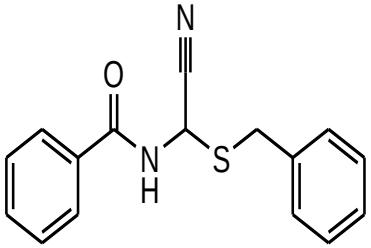

V154 (NSC 177924)

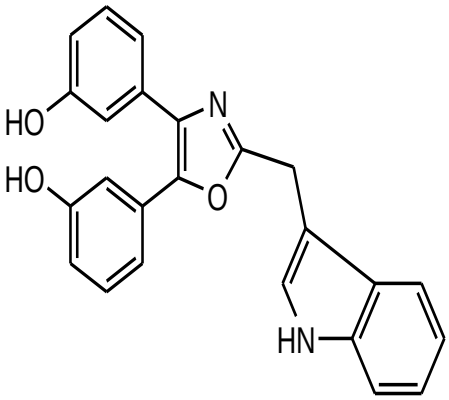

#648

Figure 3.8. Chemical structures of V131, V154 and #648.

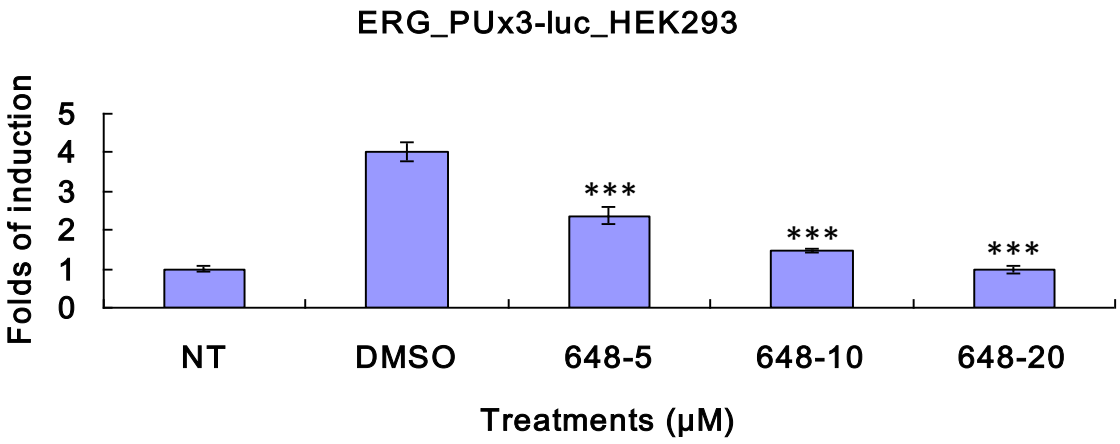

Figure 3.9. Compound #648 dose-dependently suppressed ERG-dependent luciferase activity in HEK293 cells. pMSCV-ERG, pTK-100-PUx3-Luc luciferase reporter, and Null were transfected into HEK293 cells using calcium phosphate method. NT (internal control) was transfected with empty vector pMSCV, pTK-100-PUx3-Luc and Null, and treated with DMSO. Cells were exposed to treatments for 24 hours. The experiment was repeated three times in triplicate. *** p-value < 0.0001 when compared with DMSO vehicle control.

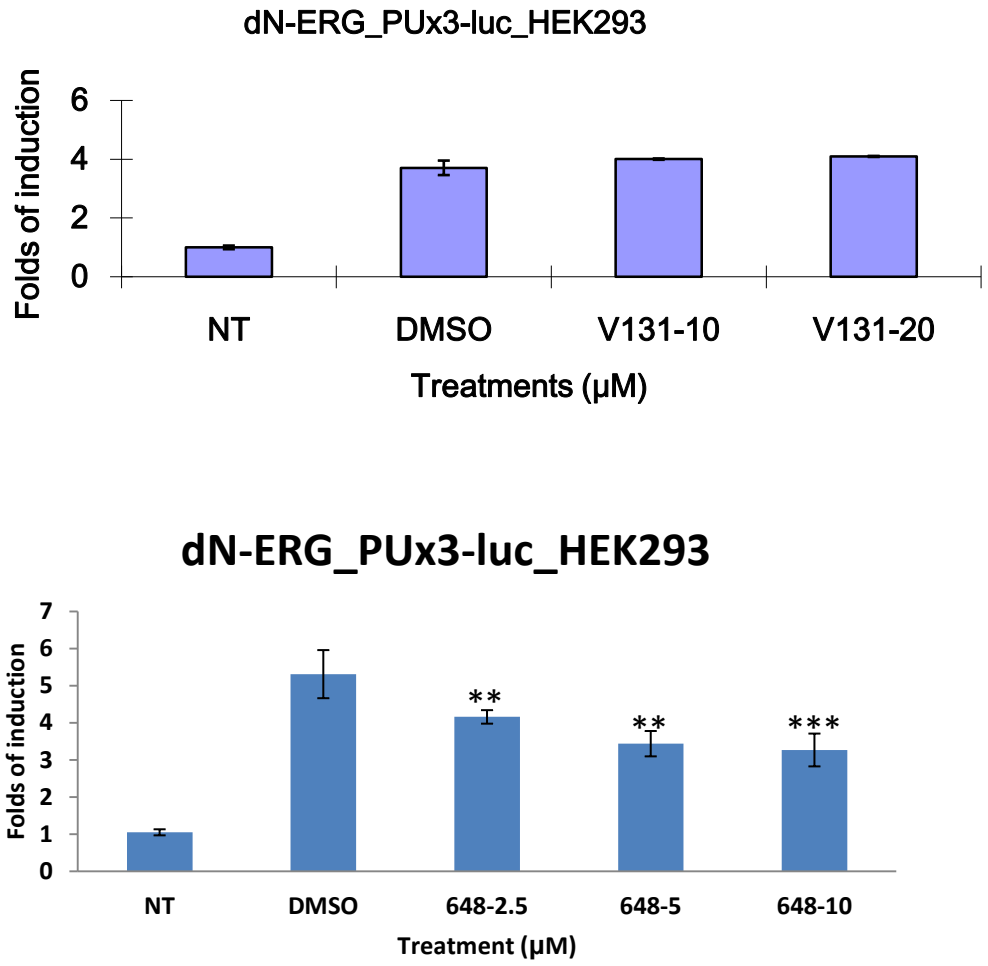

Figure 3.10. Compound #648 dose-dependently suppressed dN-ERG -dependent luciferase activity in HEK293 cells but not compound V131. pMAX deltaN-ERG, pTK-100-PUx3-Luc luciferase reporter, and Null were transfected into HEK293 using calcium phosphate method. NT (internal control) was transfected with pTK-100-PUx3-Luc luciferase reporter and Null, and treated with DMSO. Cells were exposed to treatments for 24 hours. The experiment was repeated three times in triplicate. ** p-value < 0.001 or *** p-value < 0.0001 when compared with DMSO vehicle control.

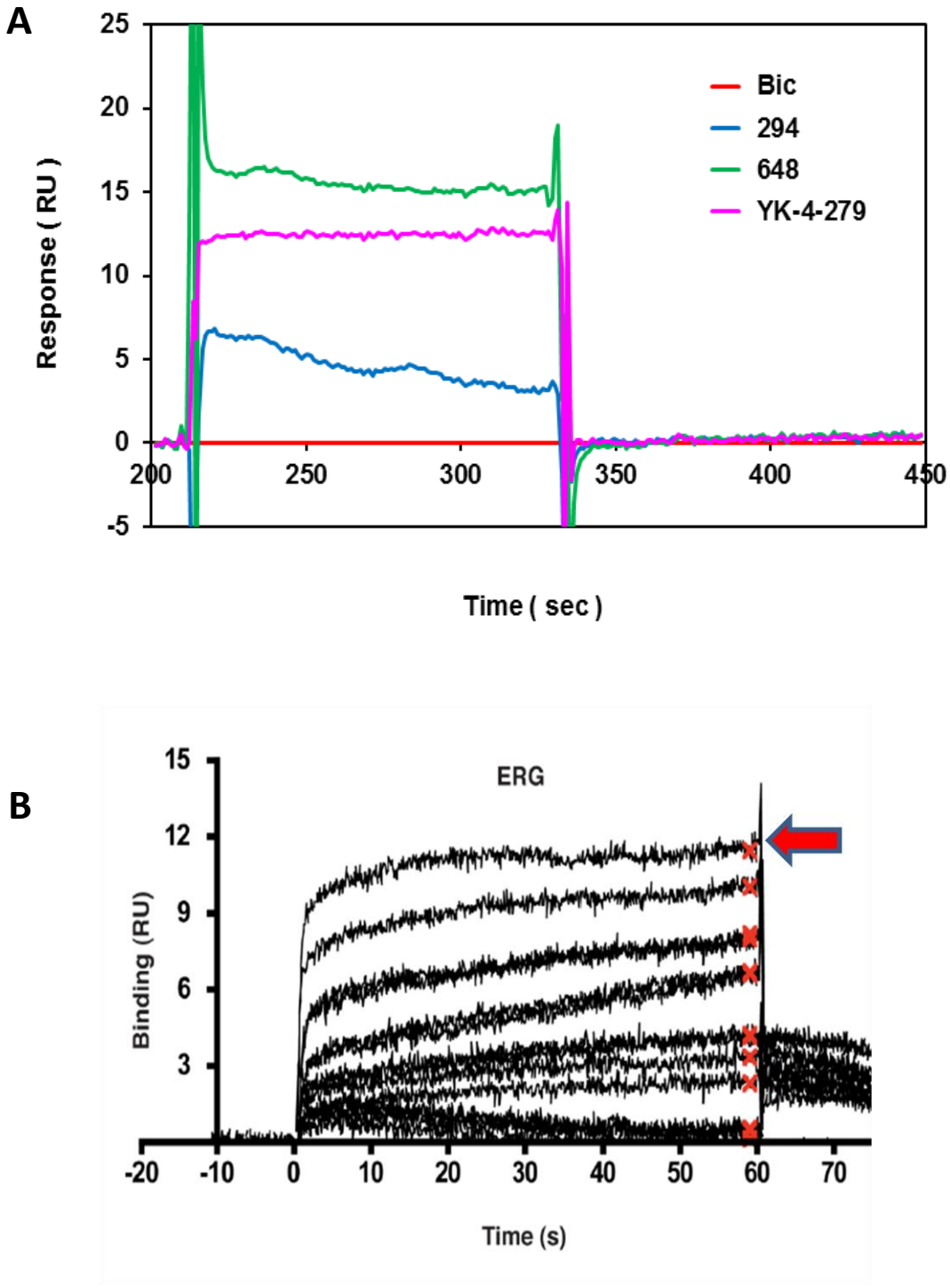

Figure 3.11. SPR analysis confirmed direct binding of #648 with ERG protein. SPR data to characterize binding specificity of **#294** and **#648** compounds at 50 μM, with a negative control (Bic) and a positive control (YK-4-279). The data indicated that **#294**, **#648** and YK-4-279 have

direct binding with ERG protein: A) Steady-state kinetics of **#294**, **#648**, YK-4-279 (positive control) and bilcalutamide (Bic) (negative control) over amine-coupled ERG surfaces with 50 μM injection (25 μL/min x 120 sec association + 120 sec dissociation); B) published titration series of YK-4-279 for comparison, taken from recent work of Rahim and co-workers [36].

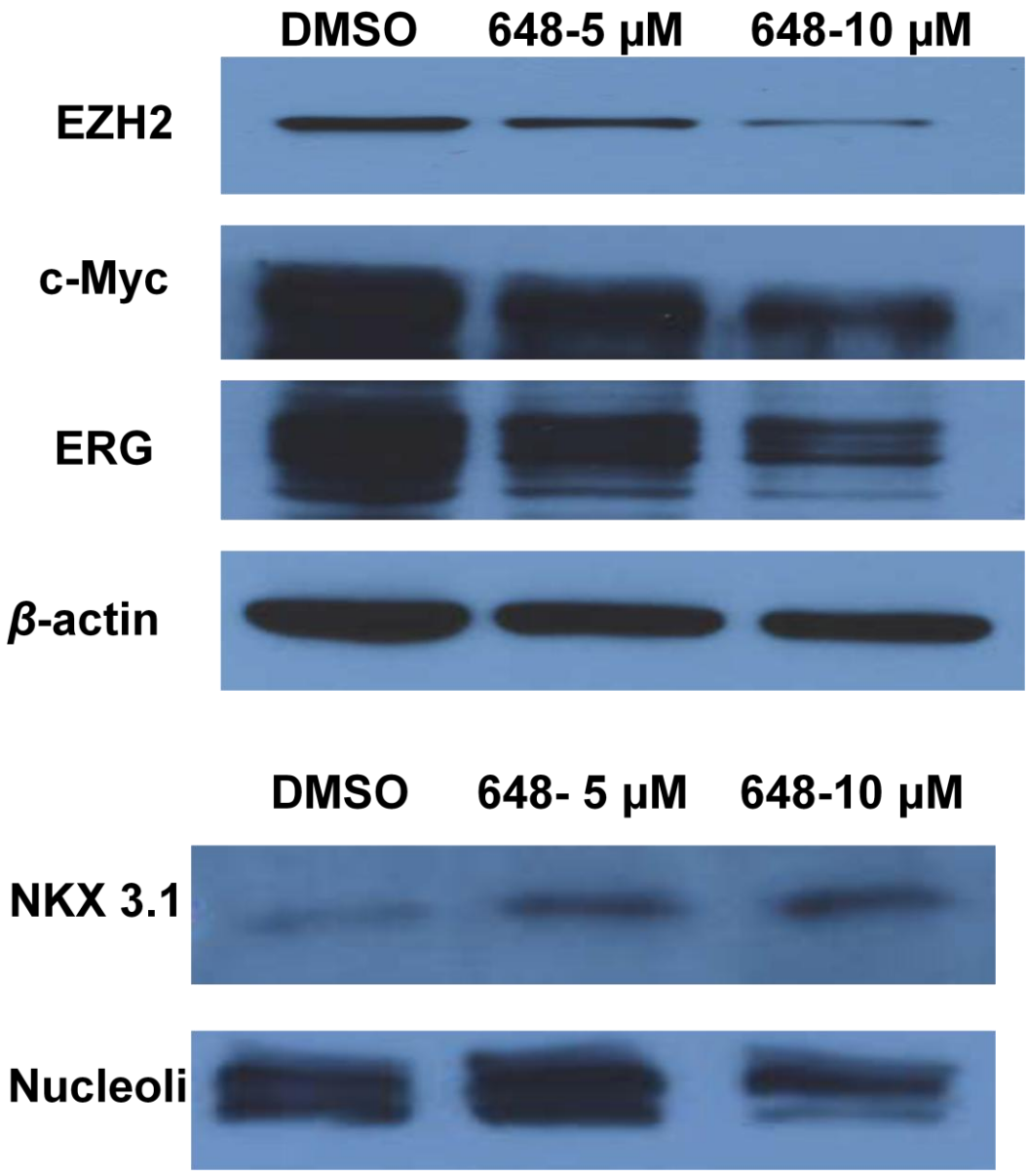

Figure 3.12. Compound #648 decreased the protein expression of ERG, EZH2 and c-Myc, and increased tumor suppressor NKX3.1 in VCaP cell. EZH2, c-Myc, and ERG decreased protein expression when the dose increased and the loading control was comparable. Tumor suppressor, NKX 3.1 showed increased expression at doses 5 µM and 10 µM and the intensity of these two bands were comparable. The cells were exposed to the treatment for 48 hours. These Western blots were repeated twice.

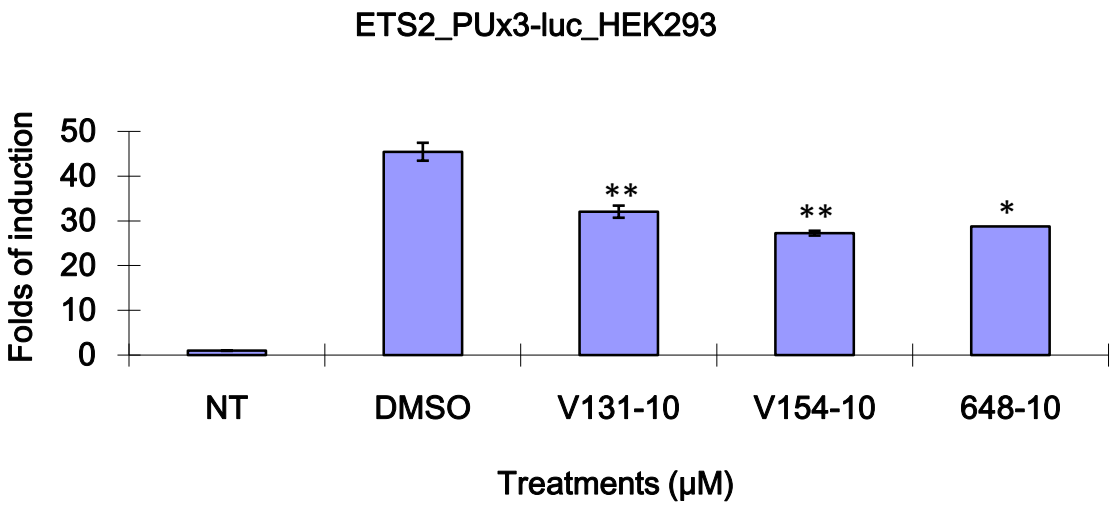

Figure 3.13. V131 and #648 suppressed ETS2-dependent luciferase activity in HEK293 cells. pcDNA 3.1-ETS2, pTK-100-PUx3-Luc luciferase reporter, and Null were transfected into HEK293 cells using calcium phosphate method. NT (internal control) was transfected with empty vector pcDNA 3.1, pTK-100-PUx3-Luc luciferase reporter and Null, and treated with DMSO. Cells were exposed to treatments for 24 hours. The experiment was repeated three times in triplicate. * p-value < 0.05 or ** p-value < 0.001 when compared with DMSO vehicle control.

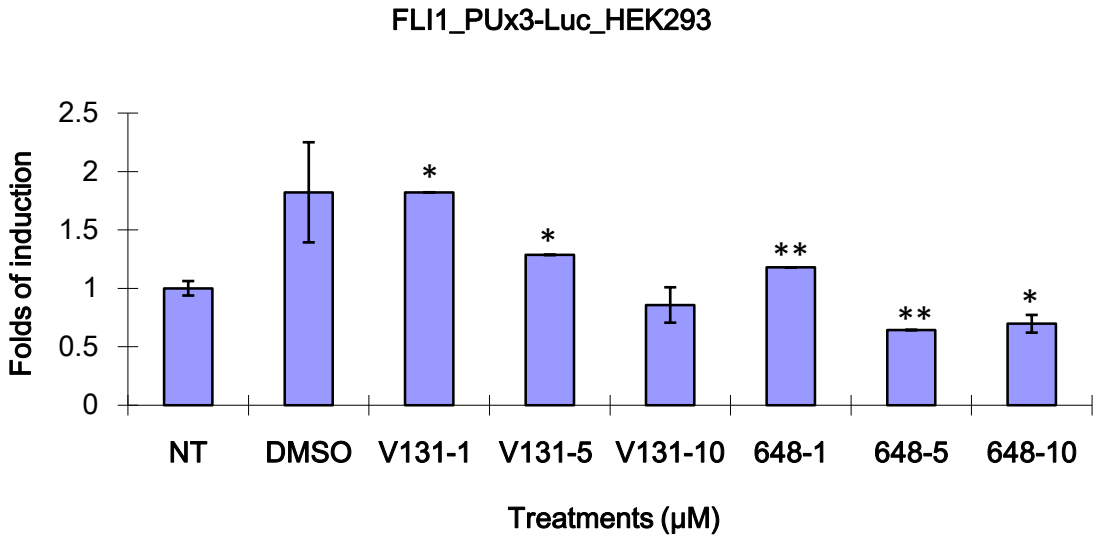

Figure 3.14. V131 and #648 dose-dependently suppressed FLI1-dependent luciferase activity in HEK293 cells. pSG5-FLI1, pTK-100-PUx3-Luc luciferase reporter, and Null were transfected into HEK293 cells using calcium phosphate method. NT (internal control) was transfected with pTK-100-PUx3-Luc and Null, and treated with DMSO. Cells were exposed to treatments for 24 hours. The experiment was repeated three times in triplicate. * p-value < 0.05 or ** p-value < 0.001 when compared with DMSO vehicle control.

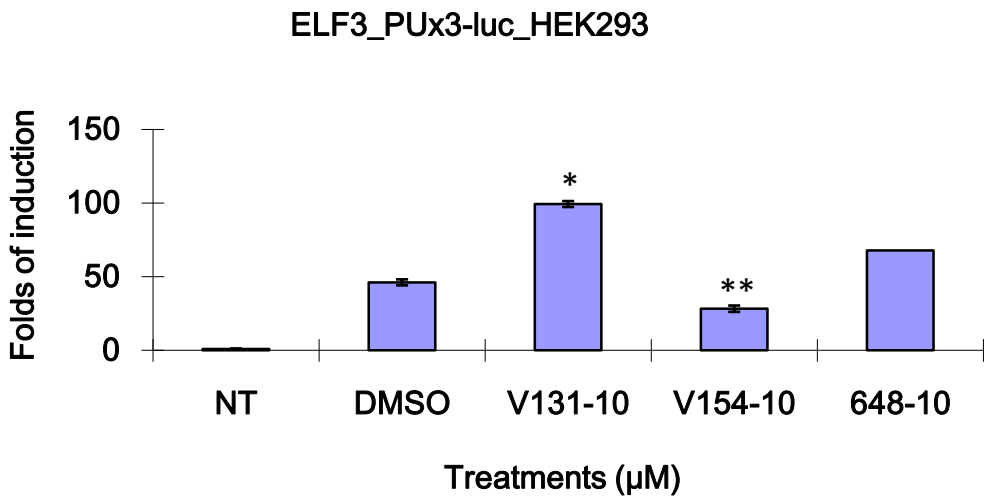

Figure 3.15. ELF3- dependent luciferase assay in HEK293 indicated V131 and #648 were inactive against ELF3, but V154 was active. pi-RES-puro-ELF3, pTK-100-PUx3-Luc luciferase reporter, and Null were transfected into HEK293 cells using calcium phosphate method. NT (internal control) was transfected with pTK-100-PUx3-Luc and Null, and treated with DMSO. The experiment was repeated three times in triplicate. * p-value < 0.05 or ** p-value < 0.001 when compared with DMSO vehicle control.

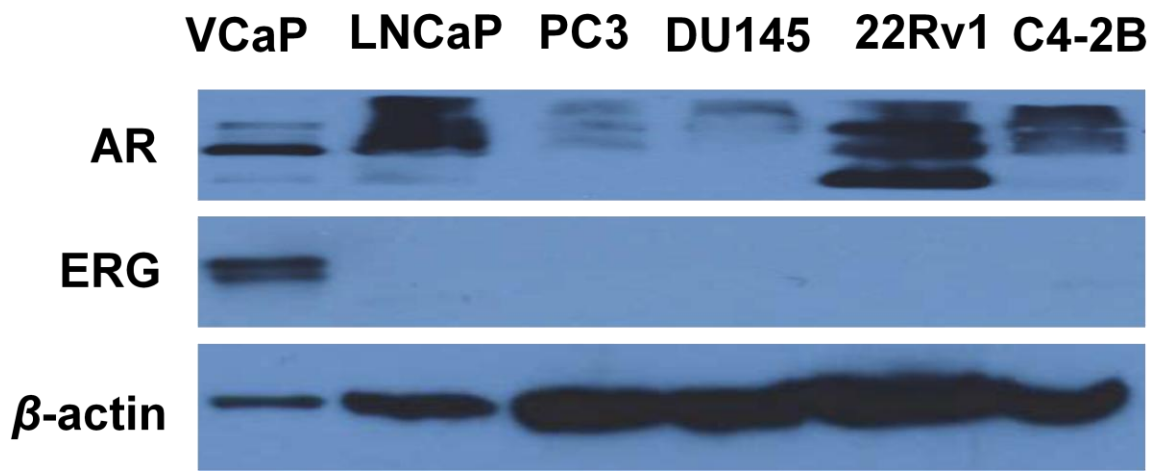

Figure 3.16. Western blot analysis to detect endogenous expression of AR and ERG in six prostate cancer cells. This experiment was repeated twice.

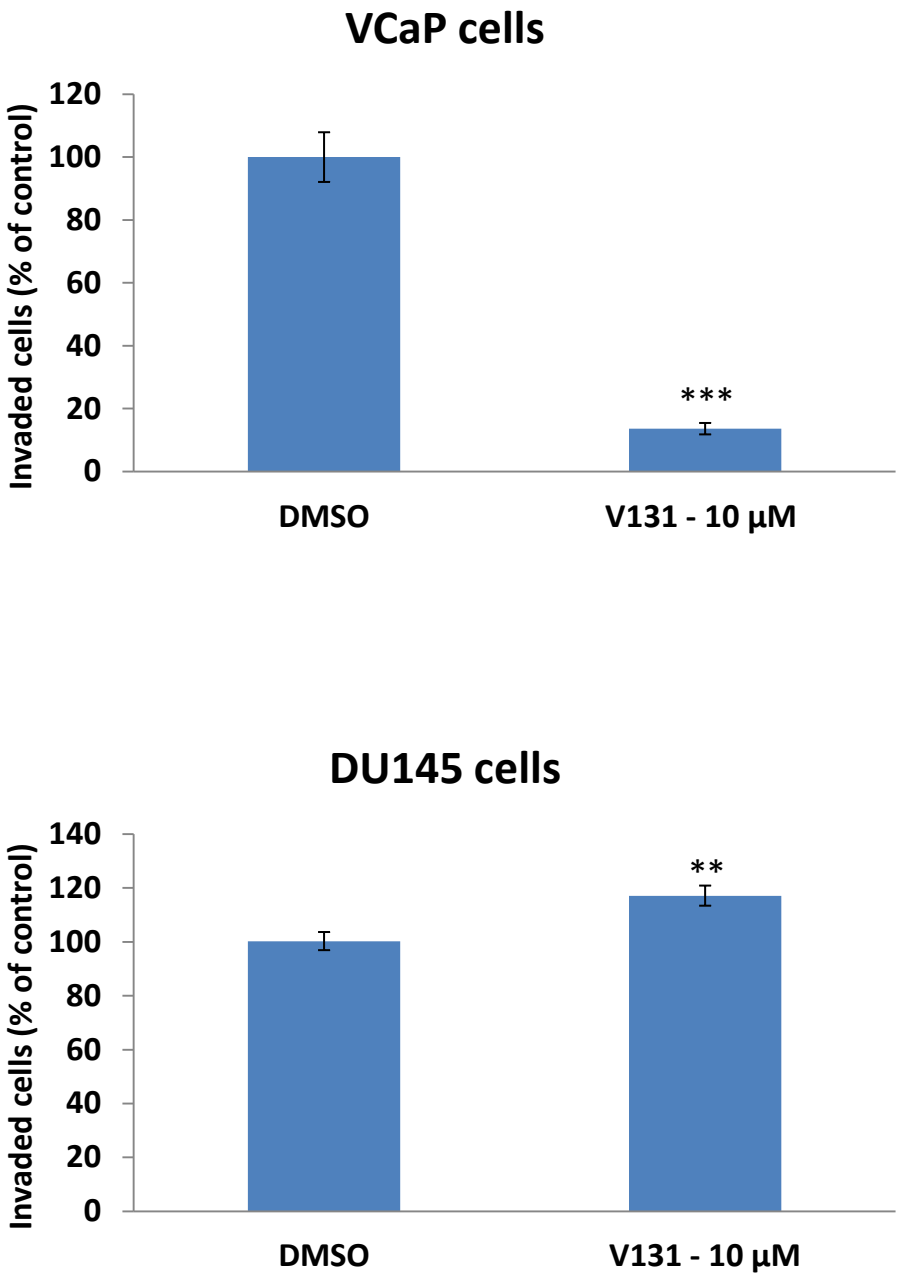

Figure 3.17. Boyden chamber invasion assay of V131 against VCaP and DU145 cells. **V131** at 10 µM inhibited invasion substantially in ERG-positive, VCaP cells but not in ERG-negative, DU145 cells after 48-hour treatment. ** p-value < 0.001, *** p-value < 0.0001 when compared with DMSO vehicle control.

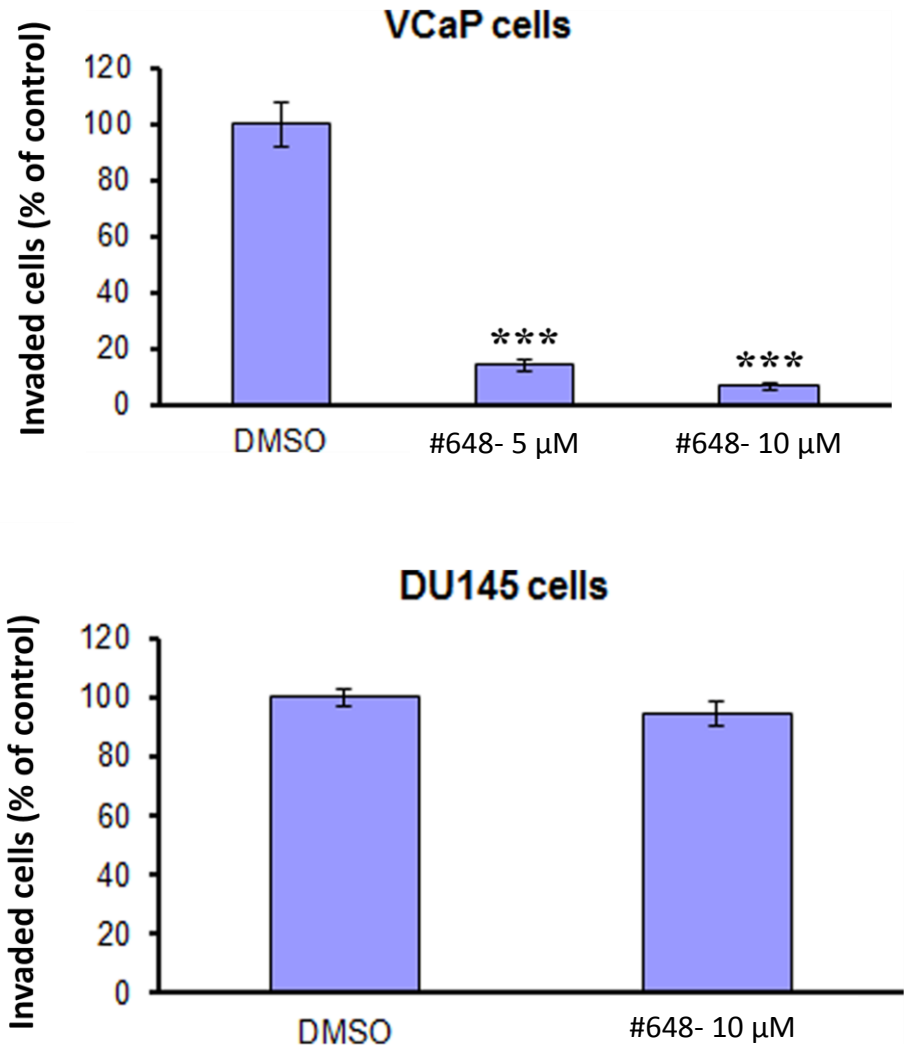

Figure 3.18. Boyden chamber invasion assay of #648 against VCaP and DU145 cells. **#648** at 10 µM inhibited invasion substantially in ERG-positive, VCaP cells but not in ERG-negative, DU145 cells after 48-hour treatment. *** p-value < 0.0001 when compared with DMSO vehicle control.

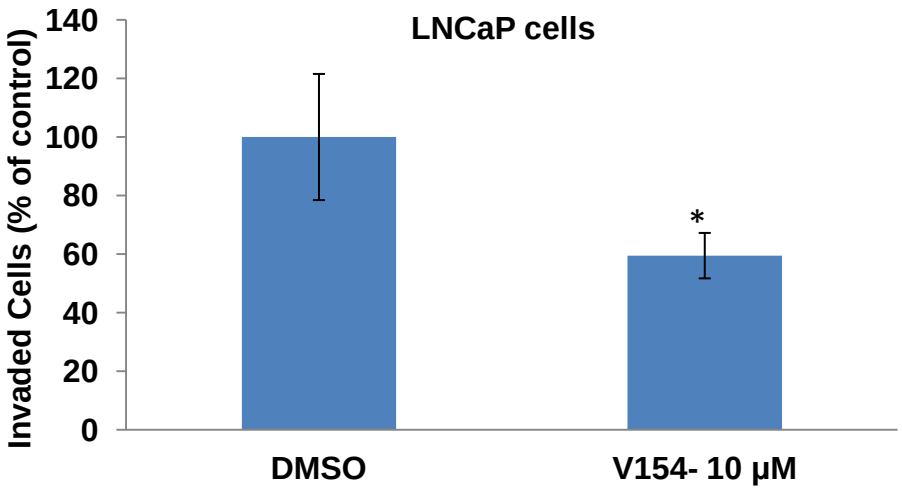

Figure 3.18. Boyden chamber invasion assay of V154 against LNCaP cells. V154 at 10 µM inhibited invasion in ETV1-positive, LNCaP cells by ~40% compared to the DMSO vehicle control after 24-hour treatment. * p-value < 0.05 when compared with DMSO vehicle control.

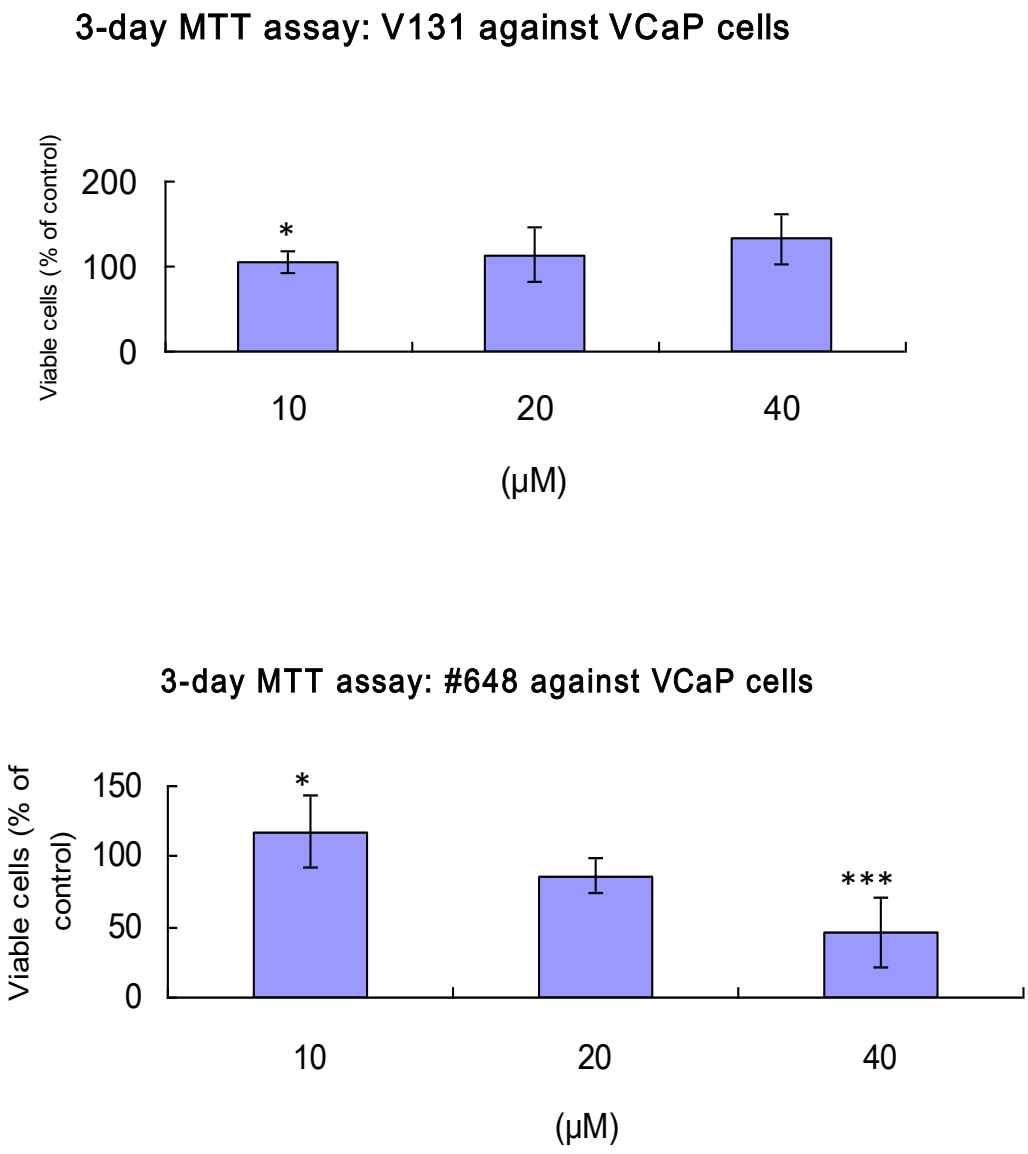

Figure 3.20. Cytotoxicity of V131 and #648 against VCaP cells. Evaluated by MTT assays for 3-day treatment time. * p-value < 0.05, ** p-value < 0.001 when compared with DMSO vehicle control.

.

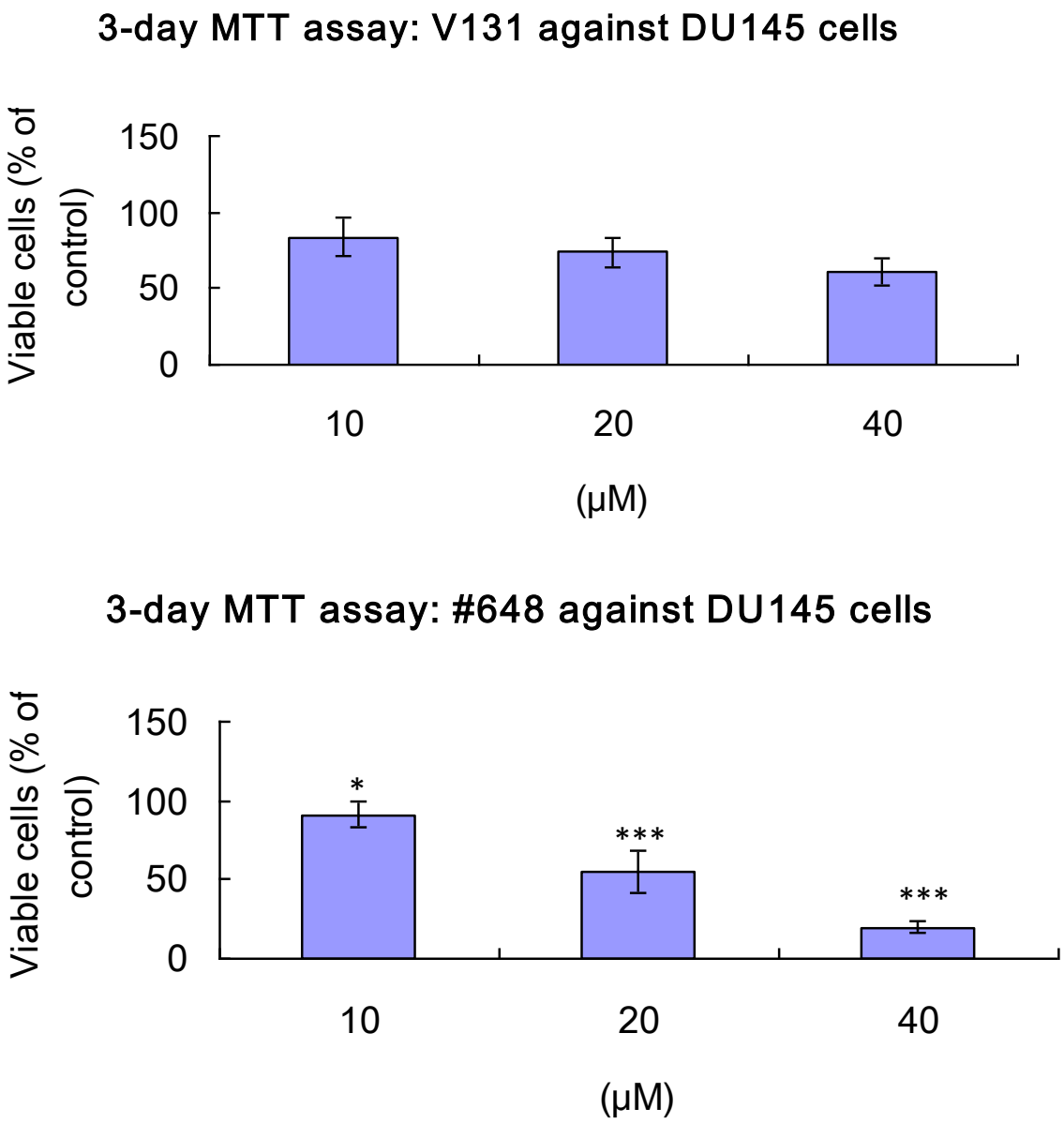

Figure 3.21. Cytotoxicity of V131 and #648 against DU145 cells. Evaluated by MTT assays for 3-day treatment time. * p-value < 0.05, ** p-value < 0.001 when compared with DMSO vehicle control.

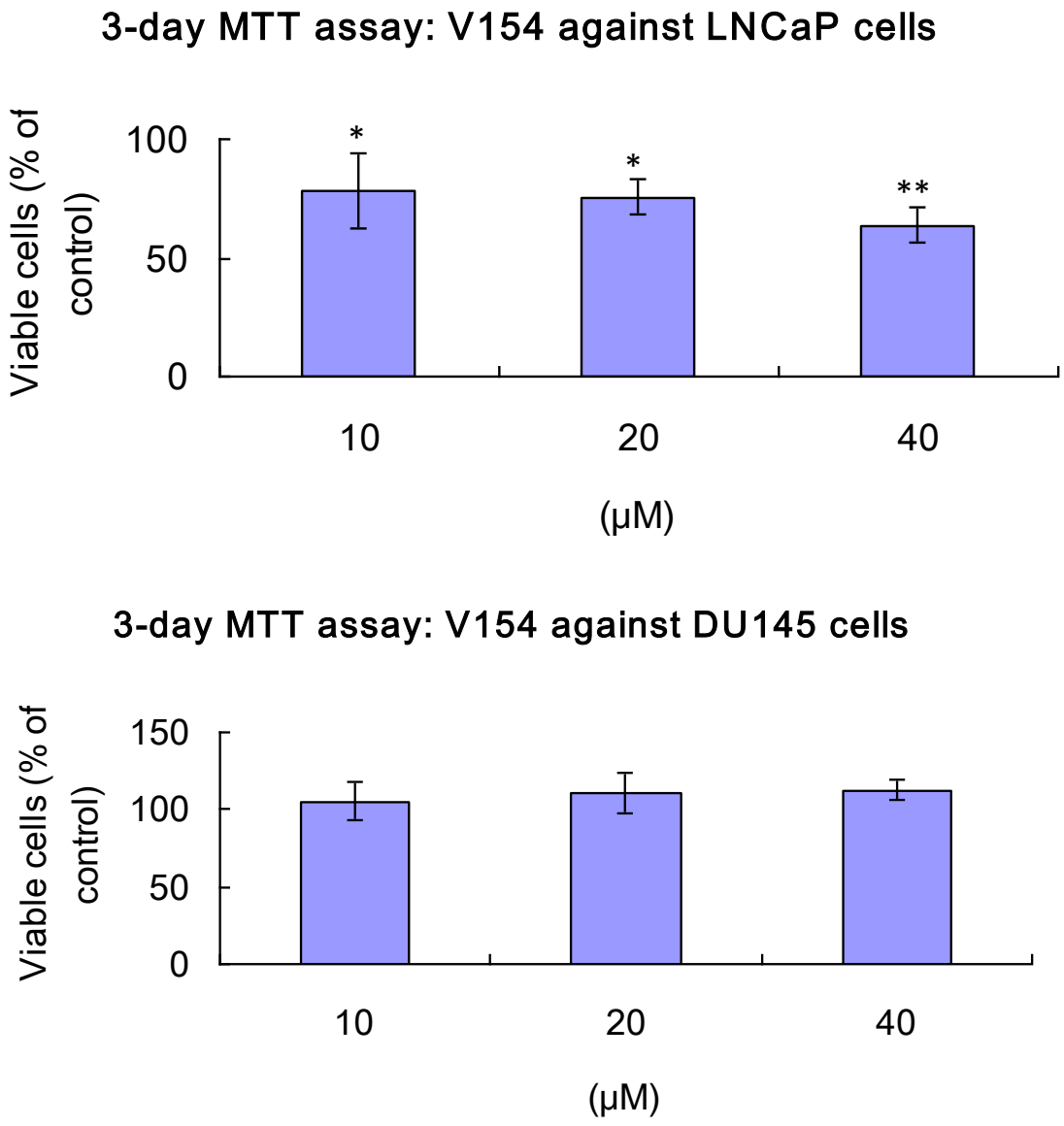

Figure 3.22. Cytotoxicity of V154 against LNCaP and DU145 cells. Evaluated by MTT assays for 3-day treatment time. * p-value < 0.05, ** p-value < 0.001 when compared with DMSO vehicle control.

REFERENCES

1. Siegel, R., D. Naishadham, and A. Jemal, *Cancer statistics, 2012.* CA: A Cancer Journal for Clinicians, 2012. **62**(1): p. 10-29.
2. Williams, H. and I.J. Powell, *Epidemiology, pathology, and genetics of prostate cancer among African Americans compared with other ethnicities.* Methods Mol Biol, 2009. **472**: p. 439-53.
3. Zeigler-Johnson, C.M., et al., *Evaluation of prostate cancer characteristics in four populations worldwide.* Can J Urol, 2008. **15**(3): p. 4056-64.
4. Martin, D.N., A.M. Starks, and S. Ambs, *Biological determinants of health disparities in prostate cancer.* Curr Opin Oncol, 2013. **25**(3): p. 235-41.
5. Kheirandish, P. and F. Chinegwundoh, *Ethnic differences in prostate cancer.* Br J Cancer, 2011. **105**(4): p. 481-5.
6. Langeberg, W.J., W.B. Isaacs, and J.L. Stanford, *Genetic etiology of hereditary prostate cancer.* Front Biosci, 2007. **12**: p. 4101-10.
7. Hoffman, R.M., *Screening for Prostate Cancer.* New England Journal of Medicine, 2011. **365**(21): p. 2013-2019.
8. Sirovich, B.E., L.M. Schwartz, and S. Woloshin, *Screening men for prostate and colorectal cancer in the United States: does practice reflect the evidence?* Jama, 2003. **289**(11): p. 1414-20.
9. Yao, S.L. and G. Lu-Yao, *Understanding and appreciating overdiagnosis in the PSA era.* J Natl Cancer Inst, 2002. **94**(13): p. 958-60.
10. Uzzo, R.G., et al., *Mechanisms of apoptosis resistance and treatment strategies to overcome them in hormone-refractory prostate cancer.* Cancer, 2008. **112**(8): p. 1660-71.
11. Damber, J.-E. and G. Aus, *Prostate cancer.* The Lancet, 2008. **371**(9625): p. 1710-1721.
12. Huggins, C. and C.V. Hodges, *Studies on prostatic cancer: I. The effect of castration, of estrogen and of androgen injection on serum phosphatases in metastatic carcinoma of the prostate.* CA: A Cancer Journal for Clinicians, 1972. **22**(4): p. 232-240.
13. Taplin, M.E. and S.M. Ho, *Clinical review 134: The endocrinology of prostate cancer.* J Clin Endocrinol Metab, 2001. **86**(8): p. 3467-77.
14. Tannock, I.F., et al., *Docetaxel plus Prednisone or Mitoxantrone plus Prednisone for Advanced Prostate Cancer.* New England Journal of Medicine, 2004. **351**(15): p. 1502-1512.
15. Petrylak, D.P., et al., *Docetaxel and estramustine compared with mitoxantrone and prednisone for advanced refractory prostate cancer.* N Engl J Med, 2004. **351**(15): p. 1513-20.
16. Eichholz, A., et al., *Putting the brakes on continued androgen receptor signaling in castration-resistant prostate cancer.* Molecular and Cellular Endocrinology, 2012. **360**(1–2): p. 68-75.
17. El-Amm, J., et al., *Metastatic Castration-Resistant Prostate Cancer: Critical Review of Enzalutamide.* Clin Med Insights Oncol, 2013. **7**: p. 235-245.
18. Tran, C., et al., *Development of a Second-Generation Antiandrogen for Treatment of Advanced Prostate Cancer.* Science, 2009. **324**(5928): p. 787-790.
19. Fizazi, K., et al., *Abiraterone acetate for treatment of metastatic castration-resistant prostate cancer: final overall survival analysis of the COU-AA-301 randomised, double-blind, placebo-controlled phase 3 study.* Lancet Oncol, 2012. **13**(10): p. 983-92.

20. Scher, H.I., et al., *Increased Survival with Enzalutamide in Prostate Cancer after Chemotherapy.* New England Journal of Medicine, 2012. **367**(13): p. 1187-1197.
21. Seruga, B. and I.F. Tannock, *Chemotherapy-based treatment for castration-resistant prostate cancer.* J Clin Oncol, 2011. **29**(27): p. 3686-94.
22. Attard, G., et al., *Antitumor activity with CYP17 blockade indicates that castration-resistant prostate cancer frequently remains hormone driven.* Cancer Res, 2009. **69**(12): p. 4937-40.
23. Attard, G., C.S. Cooper, and J.S. de Bono, *Steroid hormone receptors in prostate cancer: a hard habit to break?* Cancer Cell, 2009. **16**(6): p. 458-62.
24. Shen, H.C. and S.P. Balk, *Development of Androgen Receptor Antagonists with Promising Activity in Castration-Resistant Prostate Cancer.* Cancer Cell, 2009. **15**(6): p. 461-463.
25. Balbas, M.D., et al., *Overcoming mutation-based resistance to antiandrogens with rational drug design.* eLife, 2013. **2**.
26. Korpal, M., et al., *An F876L mutation in androgen receptor confers genetic and phenotypic resistance to MDV3100 (enzalutamide).* Cancer Discov, 2013. **3**(9): p. 1030-43.
27. Visakorpi, T., et al., *In vivo amplification of the androgen receptor gene and progression of human prostate cancer.* Nat Genet, 1995. **9**(4): p. 401-6.
28. Edwards, J., et al., *Androgen receptor gene amplification and protein expression in hormone refractory prostate cancer.* Br J Cancer, 2003. **89**(3): p. 552-6.
29. Taplin, M.E., et al., *Selection for androgen receptor mutations in prostate cancers treated with androgen antagonist.* Cancer Res, 1999. **59**(11): p. 2511-5.
30. Hara, T., et al., *Novel mutations of androgen receptor: a possible mechanism of bicalutamide withdrawal syndrome.* Cancer Res, 2003. **63**(1): p. 149-53.
31. Cai, C., et al., *Intratumoral de novo steroid synthesis activates androgen receptor in castration-resistant prostate cancer and is upregulated by treatment with CYP17A1 inhibitors.* Cancer Res, 2011. **71**(20): p. 6503-13.
32. Weber, M.J. and D. Gioeli, *Ras signaling in prostate cancer progression.* J Cell Biochem, 2004. **91**(1): p. 13-25.
33. Gregory, C.W., et al., *A mechanism for androgen receptor-mediated prostate cancer recurrence after androgen deprivation therapy.* Cancer Res, 2001. **61**(11): p. 4315-9.
34. Chan, S.C., Y. Li, and S.M. Dehm, *Androgen receptor splice variants activate androgen receptor target genes and support aberrant prostate cancer cell growth independent of canonical androgen receptor nuclear localization signal.* J Biol Chem, 2012. **287**(23): p. 19736-49.
35. Hu, R., et al., *Ligand-Independent Androgen Receptor Variants Derived from Splicing of Cryptic Exons Signify Hormone-Refractory Prostate Cancer.* Cancer Research, 2009. **69**(1): p. 16-22.
36. Eder, I.E., et al., *Targeting the androgen receptor in hormone-refractory prostate cancer--new concepts.* Future Oncol, 2005. **1**(1): p. 93-101.
37. Tomlins, S.A., et al., *Recurrent fusion of TMPRSS2 and ETS transcription factor genes in prostate cancer.* Science, 2005. **310**(5748): p. 644-8.
38. Tomlins, S.A., et al., *TMPRSS2:ETV4 gene fusions define a third molecular subtype of prostate cancer.* Cancer Res, 2006. **66**(7): p. 3396-400.
39. Tomlins, S.A., et al., *ETS gene fusions in prostate cancer: from discovery to daily clinical practice.* Eur Urol, 2009. **56**(2): p. 275-86.

40. Mehra, R., et al., *Characterization of TMPRSS2-ETS gene aberrations in androgen-independent metastatic prostate cancer.* Cancer Res, 2008. **68**(10): p. 3584-90.
41. Mosquera, J.M., et al., *Prevalence of TMPRSS2-ERG fusion prostate cancer among men undergoing prostate biopsy in the United States.* Clin Cancer Res, 2009. **15**(14): p. 4706-11.
42. Magi-Galluzzi, C., et al., *TMPRSS2-ERG gene fusion prevalence and class are significantly different in prostate cancer of Caucasian, African-American and Japanese patients.* Prostate, 2011. **71**(5): p. 489-97.
43. Lee, K., et al., *TMPRSS2-ERG gene fusion and clinicopathologic characteristics of Korean prostate cancer patients.* Urology, 2010. **76**(5): p. 1268.e7-13.
44. Miyagi, Y., et al., *ETS family-associated gene fusions in Japanese prostate cancer: analysis of 194 radical prostatectomy samples.* Mod Pathol, 2010. **23**(11): p. 1492-8.
45. Yoshimoto, M., et al., *Absence of TMPRSS2:ERG fusions and PTEN losses in prostate cancer is associated with a favorable outcome.* Mod Pathol, 2008. **21**(12): p. 1451-60.
46. Mehra, R., et al., *Comprehensive assessment of TMPRSS2 and ETS family gene aberrations in clinically localized prostate cancer.* Mod Pathol, 2007. **20**(5): p. 538-44.
47. Watson, S.K., et al., *Minimum altered regions in early prostate cancer progression identified by high resolution whole genome tiling path BAC array comparative hybridization.* Prostate, 2009. **69**(9): p. 961-75.
48. Barwick, B.G., et al., *Prostate cancer genes associated with TMPRSS2-ERG gene fusion and prognostic of biochemical recurrence in multiple cohorts.* Br J Cancer, 2010. **102**(3): p. 570-6.
49. Maroulakou, I.G. and D.B. Bowe, *Expression and function of Ets transcription factors in mammalian development: a regulatory network.* Oncogene, 2000. **19**(55): p. 6432-42.
50. Reddy, E.S., V.N. Rao, and T.S. Papas, *The erg gene: a human gene related to the ets oncogene.* Proc Natl Acad Sci U S A, 1987. **84**(17): p. 6131-5.
51. Reddy, E.S. and V.N. Rao, *erg, an ets-related gene, codes for sequence-specific transcriptional activators.* Oncogene, 1991. **6**(12): p. 2285-9.
52. Siddique, H.R., et al., *Characterization of the DNA binding and transcriptional activation domains of the erg protein.* Oncogene, 1993. **8**(7): p. 1751-5.
53. Regan, M.C., et al., *Structural and dynamic studies of the transcription factor ERG reveal DNA binding is allosterically autoinhibited.* Proc Natl Acad Sci U S A, 2013. **110**(33): p. 13374-9.
54. Kim, C.A., et al., *Polymerization of the SAM domain of TEL in leukemogenesis and transcriptional repression.* Embo j, 2001. **20**(15): p. 4173-82.
55. Mackereth, C.D., et al., *Diversity in structure and function of the Ets family PNT domains.* J Mol Biol, 2004. **342**(4): p. 1249-64.
56. Oikawa, T. and T. Yamada, *Molecular biology of the Ets family of transcription factors.* Gene, 2003. **303**: p. 11-34.
57. Dittmer, J. and A. Nordheim, *Ets transcription factors and human disease.* Biochim Biophys Acta, 1998. **1377**(2): p. F1-11.
58. Hollenhorst, P.C., L.P. McIntosh, and B.J. Graves, *Genomic and biochemical insights into the specificity of ETS transcription factors.* Annu Rev Biochem, 2011. **80**: p. 437-71.
59. Sun, C., et al., *TMPRSS2-ERG fusion, a common genomic alteration in prostate cancer activates C-MYC and abrogates prostate epithelial differentiation.* Oncogene, 2008. **27**(40): p. 5348-53.

60. Vlaeminck-Guillem, V., et al., *The Ets family member Erg gene is expressed in mesodermal tissues and neural crests at fundamental steps during mouse embryogenesis.* Mech Dev, 2000. **91**(1-2): p. 331-5.
61. Wang, J., et al., *Pleiotropic biological activities of alternatively spliced TMPRSS2/ERG fusion gene transcripts.* Cancer Res, 2008. **68**(20): p. 8516-24.
62. Dhordain, P., et al., *Mesodermal expression of the chicken erg gene associated with precartilaginous condensation and cartilage differentiation.* Mech Dev, 1995. **50**(1): p. 17-28.
63. Baltzinger, M., A.M. Mager-Heckel, and P. Remy, *Xl erg: expression pattern and overexpression during development plead for a role in endothelial cell differentiation.* Dev Dyn, 1999. **216**(4-5): p. 420-33.
64. Pham, V.N., et al., *Combinatorial function of ETS transcription factors in the developing vasculature.* Dev Biol, 2007. **303**(2): p. 772-83.
65. Loughran, S.J., et al., *The transcription factor Erg is essential for definitive hematopoiesis and the function of adult hematopoietic stem cells.* Nat Immunol, 2008. **9**(7): p. 810-9.
66. Taoudi, S., et al., *ERG dependence distinguishes developmental control of hematopoietic stem cell maintenance from hematopoietic specification.* Genes Dev, 2011. **25**(3): p. 251-62.
67. Leshem, O., et al., *TMPRSS2/ERG promotes epithelial to mesenchymal transition through the ZEB1/ZEB2 axis in a prostate cancer model.* PLoS One, 2011. **6**(7): p. e21650.
68. Sreenath, T.L., et al., *Oncogenic activation of ERG: A predominant mechanism in prostate cancer.* J Carcinog, 2011. **10**: p. 37.
69. Yu, J., et al., *An integrated network of androgen receptor, polycomb, and TMPRSS2-ERG gene fusions in prostate cancer progression.* Cancer Cell, 2010. **17**(5): p. 443-54.
70. Flajollet, S., et al., *Abnormal expression of the ERG transcription factor in prostate cancer cells activates osteopontin.* Mol Cancer Res, 2011. **9**(7): p. 914-24.
71. Kunderfranco, P., et al., *ETS transcription factors control transcription of EZH2 and epigenetic silencing of the tumor suppressor gene Nkx3.1 in prostate cancer.* PLoS One, 2010. **5**(5): p. e10547.
72. Mohamed, A.A., et al., *ERG oncogene modulates prostaglandin signaling in prostate cancer cells.* Cancer Biol Ther, 2011. **11**(4): p. 410-7.
73. Wang, J., et al., *Activation of NF-{kappa}B by TMPRSS2/ERG Fusion Isoforms through Toll-Like Receptor-4.* Cancer Res, 2011. **71**(4): p. 1325-33.
74. Nelson, W.G., A.M. De Marzo, and S. Yegnasubramanian, *Epigenetic alterations in human prostate cancers.* Endocrinology, 2009. **150**(9): p. 3991-4002.
75. Tomlins, S.A., et al., *Role of the TMPRSS2-ERG gene fusion in prostate cancer.* Neoplasia, 2008. **10**(2): p. 177-88.
76. Klezovitch, O., et al., *A causal role for ERG in neoplastic transformation of prostate epithelium.* Proceedings of the National Academy of Sciences, 2008. **105**(6): p. 2105-2110.
77. Carver, B.S., et al., *Aberrant ERG expression cooperates with loss of PTEN to promote cancer progression in the prostate.* Nat Genet, 2009. **41**(5): p. 619-24.
78. Zong, Y., et al., *ETS family transcription factors collaborate with alternative signaling pathways to induce carcinoma from adult murine prostate cells.* Proc Natl Acad Sci U S A, 2009. **106**(30): p. 12465-70.

79. Tsuzuki, S., O. Taguchi, and M. Seto, *Promotion and maintenance of leukemia by ERG.* Blood, 2011. **117**(14): p. 3858-68.
80. Salek-Ardakani, S., et al., *ERG is a megakaryocytic oncogene.* Cancer Res, 2009. **69**(11): p. 4665-73.
81. Demichelis, F., et al., *TMPRSS2:ERG gene fusion associated with lethal prostate cancer in a watchful waiting cohort.* Oncogene, 2007. **26**(31): p. 4596-9.
82. Attard, G., et al., *Duplication of the fusion of TMPRSS2 to ERG sequences identifies fatal human prostate cancer.* Oncogene, 2008. **27**(3): p. 253-63.
83. FitzGerald, L., et al., *Association of TMPRSS2-ERG gene fusion with clinical characteristics and outcomes: results from a population-based study of prostate cancer.* BMC Cancer, 2008. **8**(1): p. 1-10.
84. Perner, S., et al., *ERG rearrangement metastasis patterns in locally advanced prostate cancer.* Urology, 2010. **75**(4): p. 762-7.
85. Furusato, B., et al., *ERG oncoprotein expression in prostate cancer: clonal progression of ERG-positive tumor cells and potential for ERG-based stratification.* Prostate Cancer Prostatic Dis, 2010. **13**(3): p. 228-37.
86. Gao, X., et al., *ERG rearrangement for predicting subsequent cancer diagnosis in high-grade prostatic intraepithelial neoplasia and lymph node metastasis.* Clin Cancer Res, 2012. **18**(15): p. 4163-72.
87. Bismar, T.A., et al., *ERG protein expression reflects hormonal treatment response and is associated with Gleason score and prostate cancer specific mortality.* Eur J Cancer, 2012. **48**(4): p. 538-46.
88. Spencer, E.S., et al., *Prognostic value of ERG oncoprotein in prostate cancer recurrence and cause-specific mortality.* Prostate, 2013. **73**(9): p. 905-12.
89. Sharrocks, A.D., *The ETS-domain transcription factor family.* Nat Rev Mol Cell Biol, 2001. **2**(11): p. 827-37.
90. Bartel, F.O., T. Higuchi, and D.D. Spyropoulos, *Mouse models in the study of the Ets family of transcription factors.* Oncogene, 2000. **19**(55): p. 6443-54.
91. Remy, P. and M. Baltzinger, *The Ets-transcription factor family in embryonic development: lessons from the amphibian and bird.* Oncogene, 2000. **19**(55): p. 6417-31.
92. Paronetto, M.P., *Ewing Sarcoma Protein: A Key Player in Human Cancer.* Int J Cell Biol, 2013. **2013**: p. 642853.
93. Liu, A.Y., et al., *Identification of differentially expressed prostate genes: increased expression of transcription factor ETS-2 in prostate cancer.* Prostate, 1997. **30**(3): p. 145-53.
94. Sementchenko, V.I., et al., *ETS2 function is required to maintain the transformed state of human prostate cancer cells.* Oncogene, 1998. **17**(22): p. 2883-8.
95. Sapi, E., et al., *Ets-2 transdominant mutant abolishes anchorage-independent growth and macrophage colony-stimulating factor-stimulated invasion by BT20 breast carcinoma cells.* Cancer Res, 1998. **58**(5): p. 1027-33.
96. Neznanov, N., et al., *A single targeted Ets2 allele restricts development of mammary tumors in transgenic mice.* Cancer Res, 1999. **59**(17): p. 4242-6.
97. de Nigris, F., et al., *Induction of ETS-1 and ETS-2 transcription factors is required for thyroid cell transformation.* Cancer Res, 2001. **61**(5): p. 2267-75.
98. Shatnawi, A., et al., *ELF3 is a repressor of androgen receptor action in prostate cancer cells.* Oncogene, 2013.

99. Erkizan, H.V., et al., *A small molecule blocking oncogenic protein EWS-FLI1 interaction with RNA helicase A inhibits growth of Ewing's sarcoma.* Nat Med, 2009. **15**(7): p. 750-6.
100. Rahim, S., et al., *YK-4-279 Inhibits ERG and ETV1 Mediated Prostate Cancer Cell Invasion.* PLoS ONE, 2011. **6**(4): p. e19343.
101. Nhili, R., et al., *Targeting the DNA-binding activity of the human ERG transcription factor using new heterocyclic dithiophene diamidines.* Nucleic Acids Res, 2013. **41**(1): p. 125-38.
102. Shin, S., et al., *ETS variant 1 regulates matrix metalloproteinase-7 transcription in LNCaP prostate cancer cells.* Oncol Rep, 2013. **29**(1): p. 306-14.
103. Pellecchia, A., et al., *Overexpression of ETV4 is oncogenic in prostate cells through promotion of both cell proliferation and epithelial to mesenchymal transition.* Oncogenesis, 2012. **1**: p. e20.
104. Baena, E., et al., *ETV1 directs androgen metabolism and confers aggressive prostate cancer in targeted mice and patients.* Genes Dev, 2013. **27**(6): p. 683-98.
105. Min, J., et al., *An oncogene-tumor suppressor cascade drives metastatic prostate cancer by coordinately activating Ras and nuclear factor-kappaB.* Nat Med, 2010. **16**(3): p. 286-94.
106. Ni, M., et al., *Amplitude modulation of androgen signaling by c-MYC.* Genes Dev, 2013. **27**(7): p. 734-48.
107. Mani, R.S., et al., *TMPRSS2-ERG-mediated feed-forward regulation of wild-type ERG in human prostate cancers.* Cancer Res, 2011. **71**(16): p. 5387-92.
108. Brenner, J.C., et al., *Mechanistic Rationale for Inhibition of Poly(ADP-Ribose) Polymerase in ETS Gene Fusion-Positive Prostate Cancer.* Cancer Cell, 2011. **19**(5): p. 664-678.
109. Cai, C., et al., *ETV1 is a novel androgen receptor-regulated gene that mediates prostate cancer cell invasion.* Mol Endocrinol, 2007. **21**(8): p. 1835-46.
110. Darnell, J.E., Jr., *Transcription factors as targets for cancer therapy.* Nat Rev Cancer, 2002. **2**(10): p. 740-9.
111. Yoshida, B.A., et al., *Metastasis-suppressor genes: a review and perspective on an emerging field.* J Natl Cancer Inst, 2000. **92**(21): p. 1717-30.